

9

Visualizing Cells

Because cells are small and complex, it is hard to see their structure, hard to discover their molecular composition, and harder still to find out how their various components function. The tools at our disposal determine what we can learn about cells, and the introduction of new techniques has frequently resulted in major advances in cell biology. To understand contemporary cell biology, therefore, it is necessary to know something of its methods.

In this chapter, we briefly describe some of the principal microscopy methods used to study cells. Understanding the structural organization of cells is an essential prerequisite for learning how cells function. Optical microscopy will be our starting point because cell biology began with the light microscope, and it is still an essential tool. In recent years optical microscopy has become ever more important, largely owing to the development of methods for the specific labeling and imaging of individual cellular constituents and the reconstruction of their three-dimensional architecture. An important advantage of optical microscopy is that light is relatively nondestructive. By tagging specific cell components with fluorescent probes, such as intrinsically fluorescent proteins, we can thus watch their movement, dynamics, and interactions in living cells. Optical microscopy is limited in resolution by the wavelength of visible light. By using a beam of electrons instead, electron microscopy can image the macromolecular complexes within cells at almost atomic resolution, and in three dimensions.

Although optical microscopy and electron microscopy are important methods, it is what they have enabled scientists to discover about the structural architecture of the cell that makes them interesting. Use this chapter as a reference and read it in conjunction with the later chapters of the book rather than viewing it as an introduction to them.

LOOKING AT CELLS IN THE LIGHT MICROSCOPE

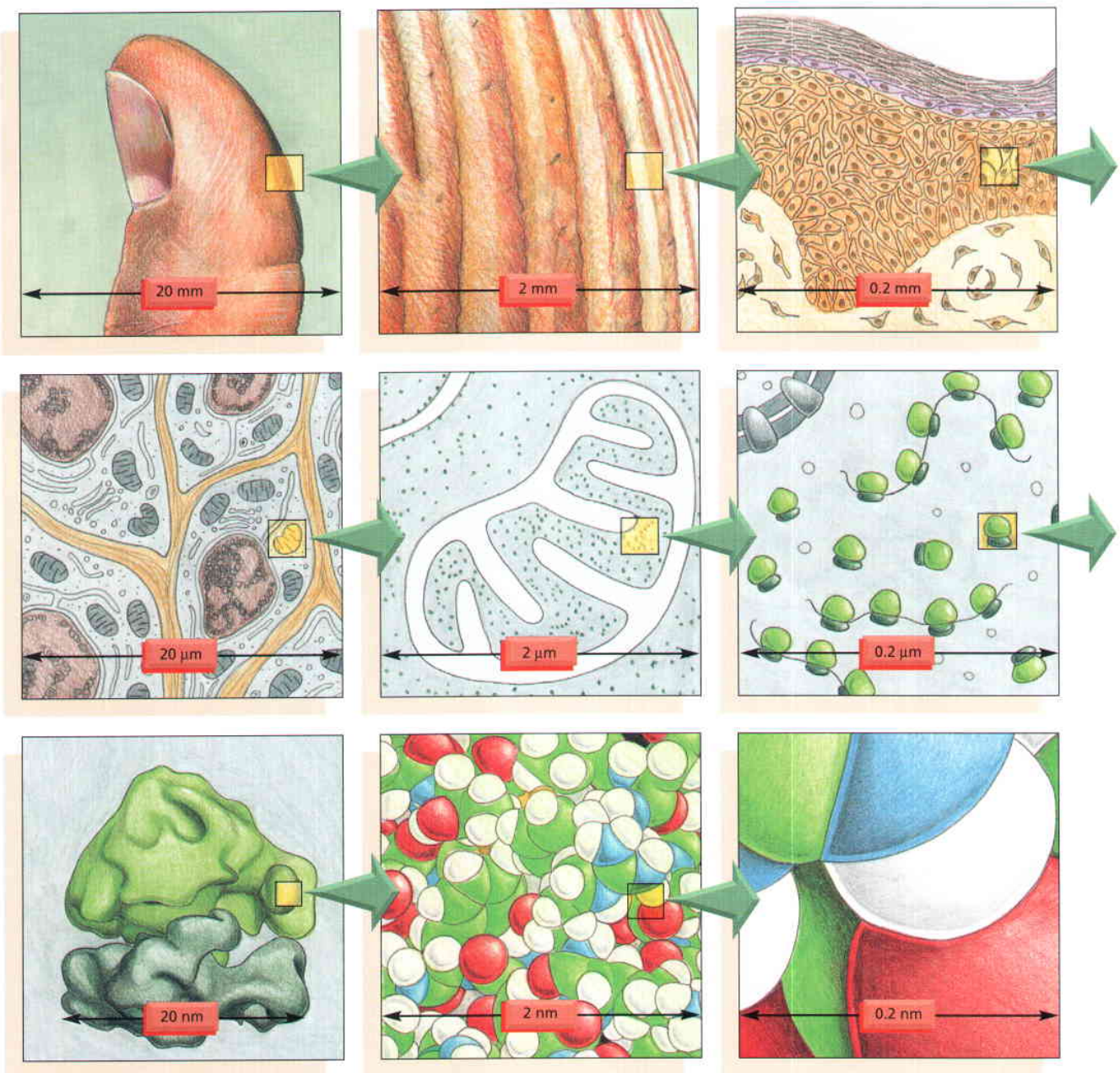
A typical animal cell is 10–20 μm in diameter, which is about one-fifth the size of the smallest particle visible to the naked eye. Only after good light microscopes became available in the early part of the nineteenth century did Schleiden and Schwann propose that all plant and animal tissues were aggregates of individual cells. Their discovery in 1838, known as the **cell doctrine**, marks the formal birth of cell biology.

Animal cells are not only tiny, but they are also colorless and translucent. Consequently, the discovery of their main internal features depended on the development, in the latter part of the nineteenth century, of a variety of stains that provided sufficient contrast to make those features visible. Similarly, the far more powerful electron microscope introduced in the early 1940s required the development of new techniques for preserving and staining cells before the full complexities of their internal fine structure could begin to emerge. To this day, microscopy relies as much on techniques for preparing the specimen as on the performance of the microscope itself. In the following discussions, we therefore consider both instruments and specimen preparation, beginning with the light microscope.

In This Chapter

LOOKING AT CELLS IN THE LIGHT MICROSCOPE 579

LOOKING AT CELLS AND MOLECULES IN THE ELECTRON MICROSCOPE 604



The series of images in **Figure 9-1** illustrate an imaginary progression from a thumb to a cluster of atoms. Each successive image represents a tenfold increase in magnification. The naked eye could see features in the first two panels, the resolution of the light microscope would extend to about the fourth panel, and the electron microscope to between about the seventh and eighth panel. **Figure 9-2** shows the sizes of various cellular and subcellular structures and the ranges of size that different types of microscopes can visualize.

The Light Microscope Can Resolve Details 0.2 μm Apart

A fundamental limitation of all microscopes is that a given type of radiation cannot be used to probe structural details much smaller than its own wavelength. The ultimate limit to the resolution of a light microscope is therefore set by the wavelength of visible light, which ranges from about 0.4 μm (for violet) to 0.7 μm

Figure 9-1 A sense of scale between living cells and atoms. Each diagram shows an image magnified by a factor of ten in an imaginary progression from a thumb, through skin cells, to a ribosome, to a cluster of atoms forming part of one of the many protein molecules in our body. Atomic details of macromolecules, as shown in the last two panels, are usually beyond the power of the electron microscope.

(for deep red). In practical terms, bacteria and mitochondria, which are about 500 nm (0.5 μm) wide, are generally the smallest objects whose shape we can clearly discern in the **light microscope**; smaller details than this are obscured by effects resulting from the wavelike nature of light. To understand why this occurs, we must follow the path of a beam of light waves as it passes through the lenses of a microscope (**Figure 9-3**).

Because of its wave nature, light does not follow exactly the idealized straight ray paths that geometrical optics predict. Instead, light waves travel through an optical system by several slightly different routes, so that they interfere with one another and cause *optical diffraction* effects. If two trains of waves reaching the same point by different paths are precisely *in phase*, with crest matching crest and trough matching trough, they will reinforce each other so as to increase brightness. In contrast, if the trains of waves are *out of phase*, they will interfere with each other in such a way as to cancel each other partly or entirely (**Figure 9-4**). The interaction of light with an object changes the phase relationships of the light waves in a way that produces complex interference effects. At high magnification, for example, the shadow of an edge that is evenly illuminated with light of uniform wavelength appears as a set of parallel lines (**Figure 9-5**), whereas that of a circular spot appears as a set of concentric rings. For the same reason, a single point seen through a microscope appears as a blurred disc, and two point objects close together give overlapping images and may merge into one. No amount of refinement of the lenses can overcome this limitation imposed by the wavelike nature of light.

The limiting separation at which two objects appear distinct—the so-called **limit of resolution**—depends on both the wavelength of the light and the *numerical aperture* of the lens system used. The numerical aperture is a measure of the width of the entry pupil of the microscope, scaled according to its distance from the object; the wider the microscope opens its eye, so to speak, the more sharply it can see (**Figure 9-6**). Under the best conditions, with violet light

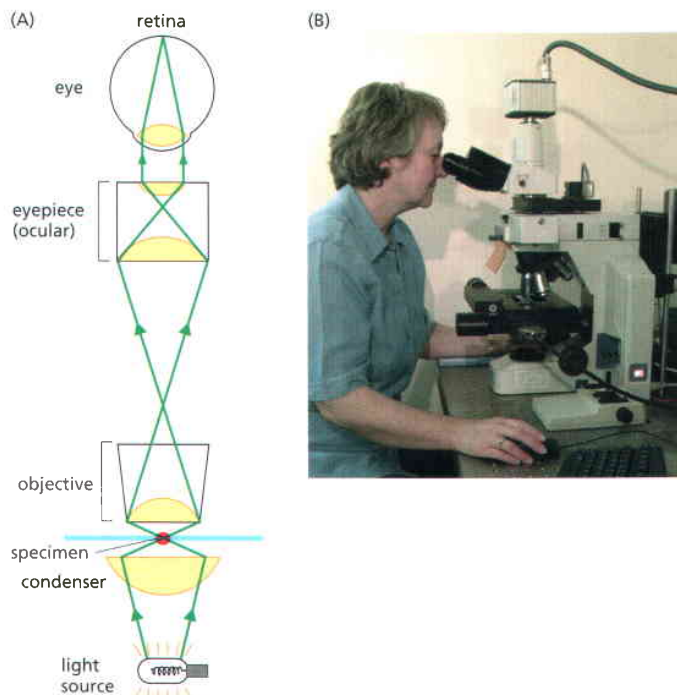


Figure 9-3 A light microscope. (A) Diagram showing the light path in a compound microscope. Light is focused on the specimen by lenses in the condenser. A combination of objective lenses and eyepiece lenses are arranged to focus an image of the illuminated specimen in the eye. (B) A modern research light microscope. (B, courtesy of Andrew Davies.)

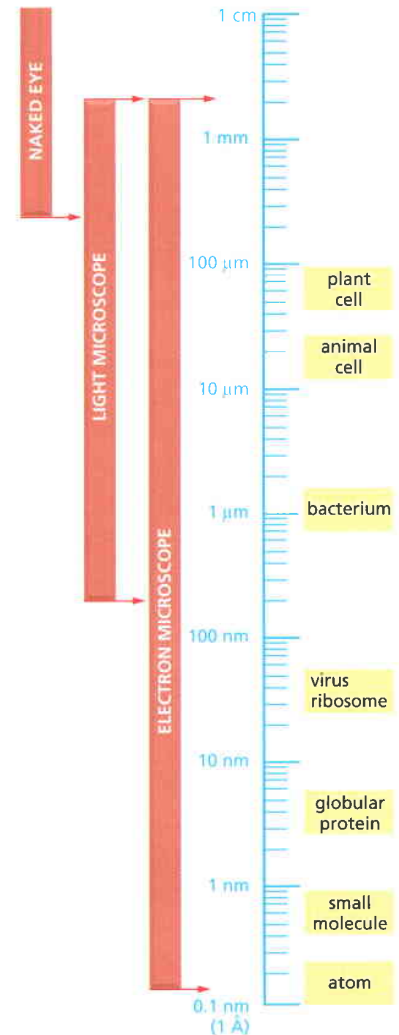


Figure 9-2 Resolving power. Sizes of cells and their components are drawn on a logarithmic scale, indicating the range of objects that can be readily resolved by the naked eye and in the light and electron microscopes. The following units of length are commonly employed in microscopy:
 μm (micrometer) = 10^{-6} m
 nm (nanometer) = 10^{-9} m
 Å (Ångström unit) = 10^{-10} m

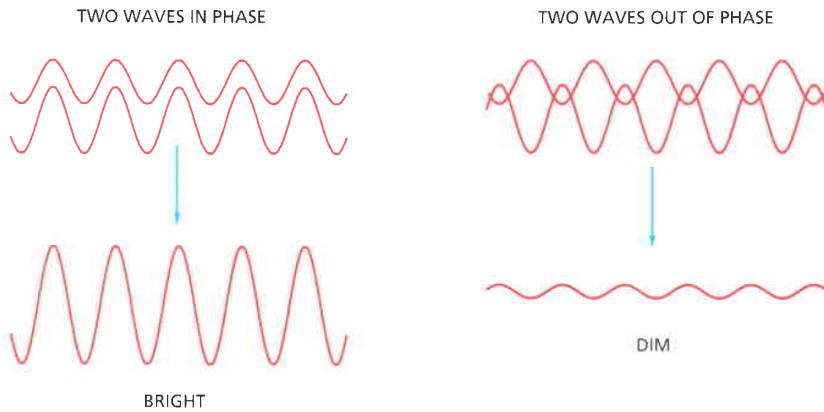


Figure 9-4 Interference between light waves. When two light waves combine in phase, the amplitude of the resultant wave is larger and the brightness is increased. Two light waves that are out of phase cancel each other partly and produce a wave whose amplitude, and therefore brightness, is decreased.

(wavelength = 0.4 μm) and a numerical aperture of 1.4, the light microscope can theoretically achieve a limit of resolution of just under 0.2 μm. Microscope makers at the end of the nineteenth century achieved this resolution and it is only rarely matched in contemporary, factory-produced microscopes. Although it is possible to *enlarge* an image as much as we want—for example, by projecting it onto a screen—it is never possible to resolve two objects in the light microscope that are separated by less than about 0.2 μm; they will appear as a single object. Notice the difference between *resolution*, discussed above, and *detection*. If a small object, below the resolution limit, itself emits light, then we may still be able to see or detect it. Thus, we can see a single fluorescently labeled microtubule even though it is about ten times thinner than the resolution limit of the light microscope. Diffraction effects, however, will cause it to appear blurred and at least 0.2 μm thick (see Figure 9-17). Because of the bright light they emit we can detect or see the stars in the night sky, even though they are far below the angular resolution of our unaided eyes. They all appear as similar points of light,

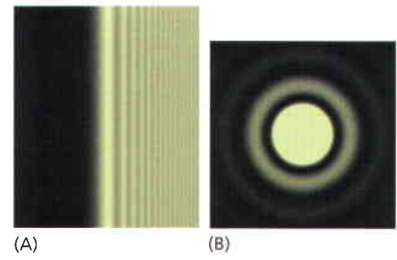


Figure 9-5 Images of an edge and of a point of light. (A) The interference effects, or fringes, seen at high magnification when light of a specific wavelength passes the edge of a solid object placed between the light source and the observer. (B) The image of a point source of light. Diffraction spreads this out into a complex, circular pattern, whose width depends on the numerical aperture of the optical system: the smaller the aperture the bigger (more blurred) the diffracted image. Two point sources can be just resolved when the center of the image of one lies on the first dark ring in the image of the other: this defines the limit of resolution.

LENSES

the **objective** lens collects a cone of light rays to create an image

the **condenser** lens focuses a cone of light rays onto each point of the specimen

RESOLUTION: the resolving power of the microscope depends on the width of the cone of illumination and therefore on both the condenser and the objective lens. It is calculated using the formula

$$\text{resolution} = \frac{0.61 \lambda}{n \sin \theta}$$

where:

- θ = half the angular width of the cone of rays collected by the objective lens from a typical point in the specimen (since the maximum width is 180°, sin θ has a maximum value of 1)
- n = the refractive index of the medium (usually air or oil) separating the specimen from the objective and condenser lenses
- λ = the wavelength of light used (for white light a figure of 0.53 μm is commonly assumed)

NUMERICAL APERTURE: $n \sin \theta$ in the equation above is called the numerical aperture of the lens (NA) and is a function of its light-collecting ability. For dry lenses this cannot be more than 1, but for oil-immersion lenses it can be as high as 1.4. The higher the numerical aperture, the greater the resolution and the brighter the image (brightness is important in fluorescence microscopy). However, this advantage is obtained at the expense of very short working distances and a very small depth of field.

Figure 9-6 Numerical aperture. The path of light rays passing through a transparent specimen in a microscope illustrates the concept of numerical aperture and its relation to the limit of resolution.

differing only in their color or brightness. Using sensitive detection methods, we can detect and follow the behavior of even a single fluorescent protein molecule with a light microscope.

We see next how we can exploit interference and diffraction to study unstained cells in the living state.

Living Cells Are Seen Clearly in a Phase-Contrast or a Differential-Interference-Contrast Microscope

Microscopists have always been challenged by the possibility that some components of the cell may be lost or distorted during specimen preparation. The only certain way to avoid the problem is to examine cells while they are alive, without fixing or freezing. For this purpose, light microscopes with special optical systems are especially useful.

When light passes through a living cell, the phase of the light wave is changed according to the cell's refractive index: a relatively thick or dense part of the cell, such as a nucleus, retards light passing through it. The phase of the light, consequently, is shifted relative to light that has passed through an adjacent thinner region of the cytoplasm. The **phase-contrast microscope** and, in a more complex way, the **differential-interference-contrast microscope** exploit the interference effects produced when these two sets of waves recombine, thereby creating an image of the cell's structure (**Figure 9-7**). Both types of light microscopy are widely used to visualize living cells. <TCAA>

A simpler way to see some of the features of a living cell is to observe the light that is scattered by its various components. In the **dark-field microscope**, the illuminating rays of light are directed from the side so that only scattered light enters the microscope lenses. Consequently, the cell appears as a bright object against a dark background. With a normal **bright-field microscope**, light passing through a cell in culture forms the image directly. **Figure 9-8** compares images of the same cell obtained by four kinds of light microscopy.

Phase-contrast, differential-interference-contrast, and dark-field microscopy make it possible to watch the movements involved in such processes as mitosis and cell migration. Since many cellular motions are too slow to be seen in real time, it is often helpful to make time-lapse movies. Here, the camera records successive frames separated by a short time delay, so that when the resulting picture series is played at normal speed, events appear greatly speeded up.

Images Can Be Enhanced and Analyzed by Digital Techniques

In recent years electronic, or digital, imaging systems, and the associated technology of **image processing**, have had a major impact on light microscopy. Certain practical limitations of microscopes, relating to imperfections in the optical

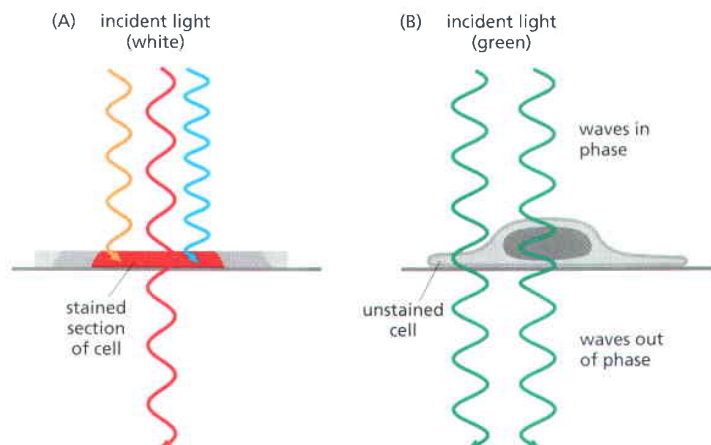


Figure 9-7 Two ways to obtain contrast in light microscopy. (A) The stained portion of the cell will absorb light of some wavelengths, which depend on the stain, but will allow other wavelengths to pass through it. A colored image of the cell is thereby obtained that is visible in the normal bright-field light microscope. (B) Light passing through the unstained, living cell experiences very little change in amplitude, and the structural details cannot be seen even if the image is highly magnified. The phase of the light, however, is altered by its passage through either thicker or denser parts of the cell, and small phase differences can be made visible by exploiting interference effects using a phase-contrast or a differential-interference-contrast microscope.

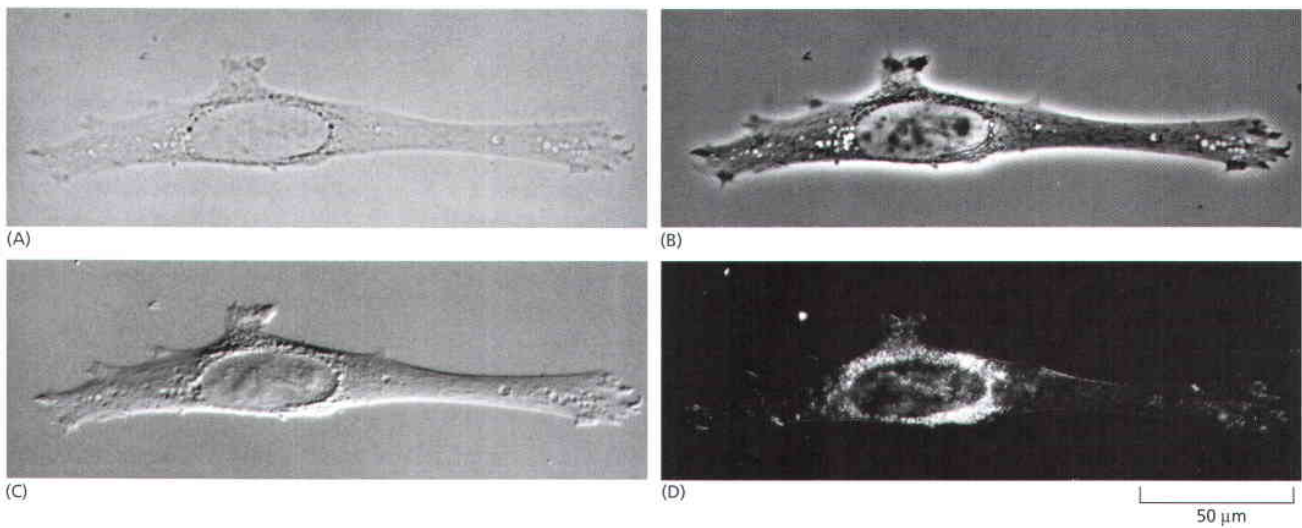


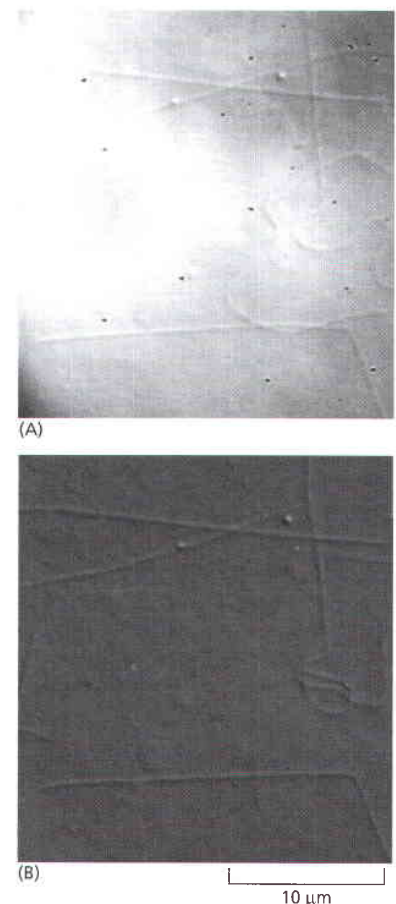
Figure 9-8 Four types of light microscopy. Four images are shown of the same fibroblast cell in culture. All images can be obtained with most modern microscopes by interchanging optical components. (A) Bright-field microscopy. (B) Phase-contrast microscopy. (C) Nomarski differential-interference-contrast microscopy. (D) Dark-field microscopy.

system have been largely overcome. Electronic imaging systems have also circumvented two fundamental limitations of the human eye: the eye cannot see well in extremely dim light, and it cannot perceive small differences in light intensity against a bright background. To increase our ability to observe cells in low light conditions, we can attach a sensitive digital camera to a microscope. These cameras contain a charge-coupled device (CCD), similar to those found in consumer digital cameras. Such CCD cameras are often cooled to reduce image noise. It is then possible to observe cells for long periods at very low light levels, thereby avoiding the damaging effects of prolonged bright light (and heat). Such low-light cameras are especially important for viewing fluorescent molecules in living cells, as explained below.

Because images produced by CCD cameras are in electronic form, they can be readily digitized, fed to a computer, and processed in various ways to extract latent information. Such image processing makes it possible to compensate for various optical faults in microscopes to attain the theoretical limit of resolution. Moreover, by digital image processing, contrast can be greatly enhanced to overcome the eye's limitations in detecting small differences in light intensity. Although this processing also enhances the effects of random background irregularities in the optical system, digitally subtracting an image of a blank area of the field removes such defects. This procedure reveals small transparent objects that were previously impossible to distinguish from the background.

The high contrast attainable by computer-assisted differential-interference-contrast microscopy makes it possible to see even very small objects such as single microtubules (**Figure 9-9**), which have a diameter of $0.025\ \mu\text{m}$, less than one-tenth the wavelength of light. Individual microtubules can also be seen in a fluorescence microscope if they are fluorescently labeled (see **Figure 9-15**). In both cases, however, the unavoidable diffraction effects badly blur the image so that the microtubules appear at least $0.2\ \mu\text{m}$ wide, making it impossible to distinguish a single microtubule from a bundle of several microtubules.

Figure 9-9 Image processing. (A) Unstained microtubules are shown here in an unprocessed digital image, captured using differential-interference-contrast microscopy. (B) The image has now been processed, first by digitally subtracting the unevenly illuminated background, and second by digitally enhancing the contrast. The result of this image processing is a picture that is easier to interpret. Note that the microtubules are dynamic and some have changed length or position between the before-and-after images. (Courtesy of Viki Allan.)



Intact Tissues Are Usually Fixed and Sectioned before Microscopy

Because most tissue samples are too thick for their individual cells to be examined directly at high resolution, they must be cut into very thin transparent slices, or *sections*. To first immobilize, kill, and preserve the cells within the tissue they must be treated with a *fixative*. Common fixatives include formaldehyde and glutaraldehyde, which form covalent bonds with the free amino groups of proteins, cross-linking them so they are stabilized and locked into position.

Because tissues are generally soft and fragile, even after fixation, they need to be embedded in a supporting medium before sectioning. The usual embedding media are waxes or resins. In liquid form these media both permeate and surround the fixed tissue; they can then be hardened (by cooling or by polymerization) to form a solid block, which is readily sectioned with a microtome. This is a machine with a sharp blade that operates like a meat slicer (**Figure 9–10**). The sections (typically 1–10 μm thick) are then laid flat on the surface of a glass microscope slide.

There is little in the contents of most cells (which are 70% water by weight) to impede the passage of light rays. Thus, most cells in their natural state, even if fixed and sectioned, are almost invisible in an ordinary light microscope. There are three main approaches to working with thin tissue sections that reveal the cells themselves or specific components within them.

First, and traditionally, sections can be stained with organic dyes that have some specific affinity for particular subcellular components. The dye *hematoxylin*, for example, has an affinity for negatively charged molecules and therefore reveals the distribution of DNA, RNA, and acidic proteins in a cell (**Figure 9–11**). The chemical basis for the specificity of many dyes, however, is not known.

Second, sectioned tissues can be used to visualize specific patterns of differential gene expression. *In situ* hybridization, discussed earlier (p. 573), reveals the cellular distribution and abundance of specific expressed RNA molecules in sectioned material or in whole mounts of small organisms or organs (**Figure 9–12**). A third and very sensitive approach, generally and widely applicable for localizing proteins of interest, depends on using fluorescent probes and markers, as we explain next.

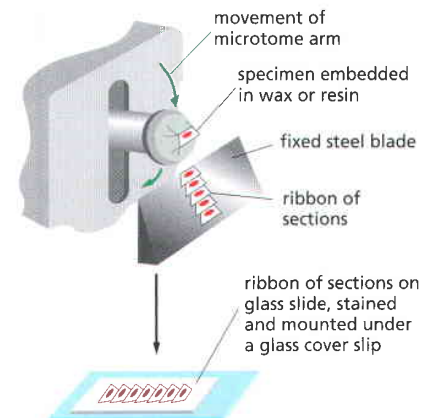


Figure 9–10 Making tissue sections. This illustration shows how an embedded tissue is sectioned with a microtome in preparation for examination in the light microscope.

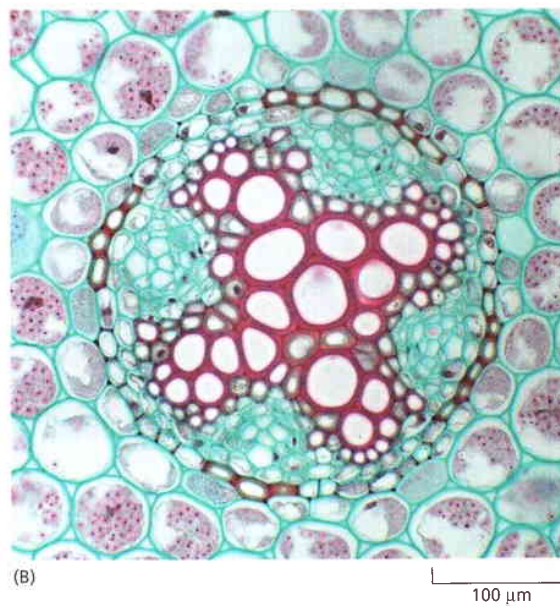
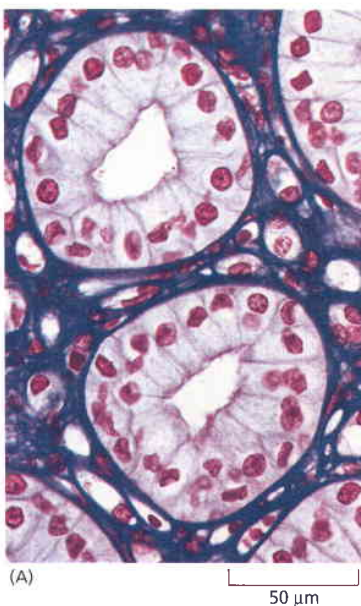


Figure 9–11 Staining of cellular components. (A) This section of cells in the urine-collecting ducts of the kidney was stained with a combination of dyes, hematoxylin and eosin, commonly used in histology. Each duct is made of closely packed cells (with nuclei stained red) that form a ring. The ring is surrounded by extracellular matrix, stained purple. (B) This section of a young plant root is stained with two dyes, safranin and fast green. The fast green stains the cellulose cell walls while the safranin stains the lignified xylem cell walls bright red. (A, from P.R. Wheater et al., *Functional Histology*, 2nd ed. London: Churchill Livingstone, 1987; B, courtesy of Stephen Grace.)

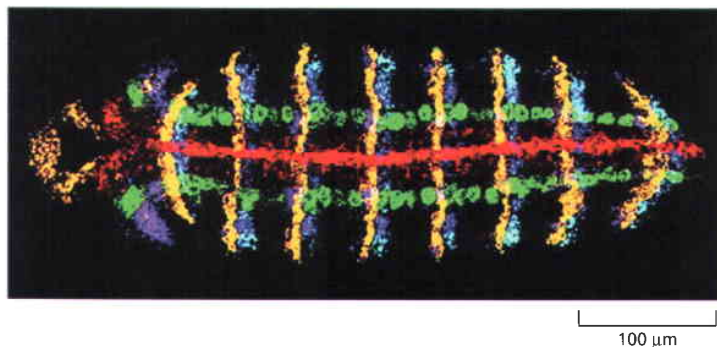


Figure 9-12 RNA *in situ* hybridization. As described in chapter 8 (see Figure 8-71), it is possible to visualize the distribution of different RNAs in tissues using *in situ* hybridization. Here, the transcription pattern of five different genes involved in patterning the early fly embryo is revealed in a single embryo. Each RNA probe has been fluorescently labeled in a different way, some directly and some indirectly, and the resulting images false-colored and combined to see each individual transcript most clearly. The genes whose expression pattern is revealed here are *wingless* (yellow), *engrailed* (blue), *short gastrulation* (red), *intermediate neuroblasts defective* (green), and *muscle specific homeobox* (purple). (From D. Kosman et al., *Science* 305:846, 2004. With permission from AAAS.)

Specific Molecules Can Be Located in Cells by Fluorescence Microscopy

Fluorescent molecules absorb light at one wavelength and emit it at another, longer wavelength. If we illuminate such a compound at its absorbing wavelength and then view it through a filter that allows only light of the emitted wavelength to pass, it will glow against a dark background. Because the background is dark, even a minute amount of the glowing fluorescent dye can be detected. The same number of molecules of an ordinary stain viewed conventionally would be practically invisible because the molecules would give only the faintest tinge of color to the light transmitted through this stained part of the specimen.

The fluorescent dyes used for staining cells are visualized with a **fluorescence microscope**. This microscope is similar to an ordinary light microscope except that the illuminating light, from a very powerful source, is passed through two sets of filters—one to filter the light before it reaches the specimen and one to filter the light obtained from the specimen. The first filter passes only the wavelengths that excite the particular fluorescent dye, while the second filter blocks out this light and passes only those wavelengths emitted when the dye fluoresces (Figure 9-13).

Fluorescence microscopy is most often used to detect specific proteins or other molecules in cells and tissues. A very powerful and widely used technique is to couple fluorescent dyes to antibody molecules, which then serve as highly specific and versatile staining reagents that bind selectively to the particular macromolecules they recognize in cells or in the extracellular matrix. Two fluorescent dyes that have been commonly used for this purpose are *fluorescein*, which emits an intense green fluorescence when excited with blue light, and

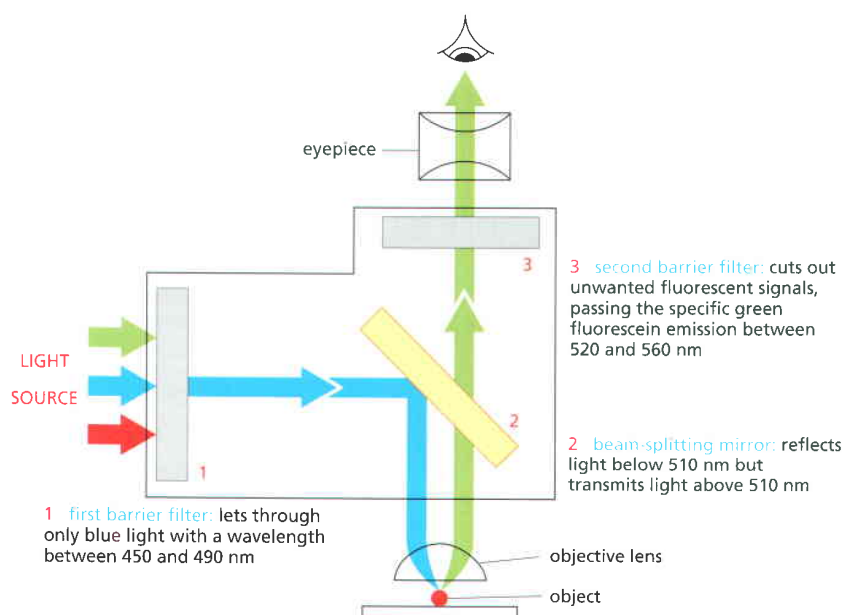


Figure 9-13 The optical system of a fluorescence microscope. A filter set consists of two barrier filters (1 and 3) and a dichroic (beam-splitting) mirror (2). This example shows the filter set for detection of the fluorescent molecule fluorescein. High-numerical-aperture objective lenses are especially important in this type of microscopy because, for a given magnification, the brightness of the fluorescent image is proportional to the fourth power of the numerical aperture (see also Figure 9-6).

Figure 9–14 Fluorescent probes. The maximum excitation and emission wavelengths of several commonly used fluorescent probes are shown in relation to the corresponding colors of the spectrum. The photon emitted by a fluorescent molecule is necessarily of lower energy (longer wavelength) than the photon absorbed and this accounts for the difference between the excitation and emission peaks. CFP, GFP, YFP and RFP are cyan, green, yellow and red fluorescent proteins respectively. These are not dyes, and are discussed in detail later in the chapter. DAPI is widely used as a general fluorescent DNA probe, which absorbs UV light and fluoresces bright blue. FITC is an abbreviation for fluorescein isothiocyanate, a widely used derivative of fluorescein, which fluoresces bright green. The other probes are all commonly used to fluorescently label antibodies and other proteins.

rhodamine, which emits a deep red fluorescence when excited with green–yellow light (Figure 9–14). By coupling one antibody to fluorescein and another to rhodamine, the distributions of different molecules can be compared in the same cell; the two molecules are visualized separately in the microscope by switching back and forth between two sets of filters, each specific for one dye. As shown in Figure 9–15, three fluorescent dyes can be used in the same way to distinguish between three types of molecules in the same cell. Many newer fluorescent dyes, such as Cy3, Cy5, and the Alexa dyes, have been specifically developed for fluorescence microscopy (see Figure 9–14). These organic fluorochromes have some disadvantages. They are excited only by light of precise, but different, wavelengths, and additionally they fade fairly rapidly when continuously illuminated. More stable inorganic fluorochromes have recently been developed, however. Tiny crystals of semiconductor material, called nanoparticles, or *quantum dots*, can all be excited to fluoresce by a broad spectrum of blue light. Their emitted light has a color that depends on the exact size of the nanocrystal, between 2 and 10 nm in diameter, and additionally the fluorescence fades only slowly with time (Figure 9–16). These nanoparticles, when coupled to other probes such as antibodies, are therefore ideal for tracking molecules over time. If introduced into a living cell, in an embryo for example, the progeny of that cell can be followed many days later by their fluorescence, allowing cell lineages to be tracked.

Fluorescence microscopy methods, discussed later in the chapter, can be used to monitor changes in the concentration and location of specific molecules inside *living* cells (see p. 592).

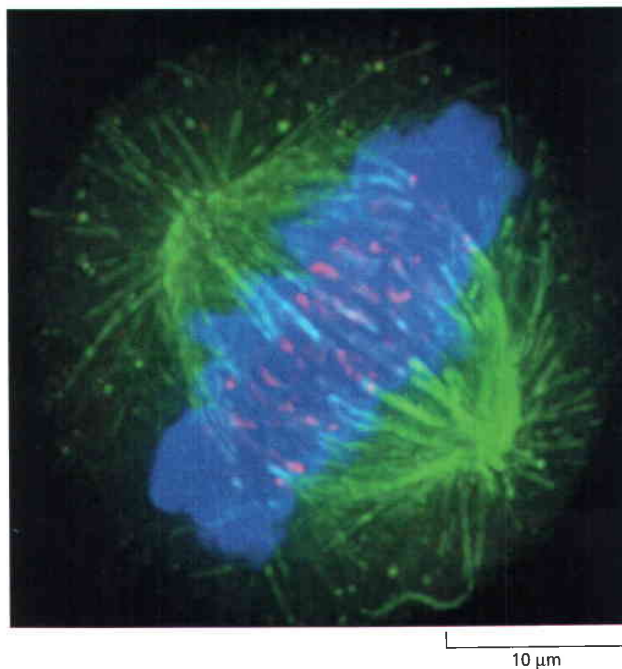
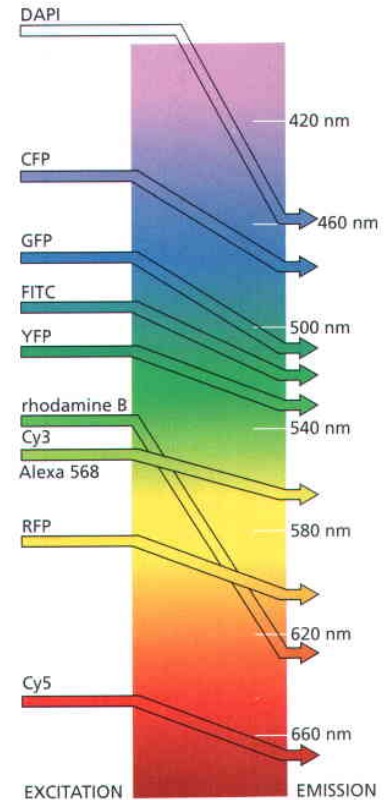


Figure 9–15 Multiple-fluorescent-probe microscopy. In this composite micrograph of a cell in mitosis, three different fluorescent probes have been used to stain three different cellular components. The spindle microtubules are revealed with a green fluorescent antibody, centromeres with a red fluorescent antibody and the DNA of the condensed chromosomes with the blue fluorescent dye DAPI. (Courtesy of Kevin F. Sullivan.)

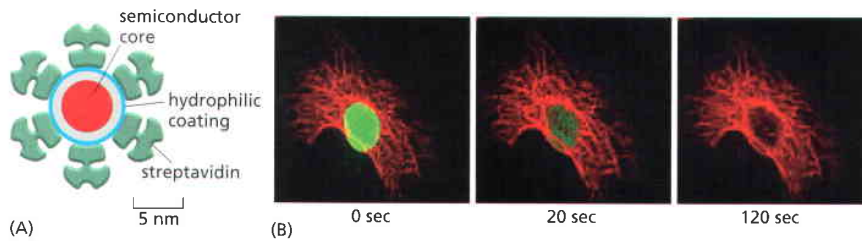


Figure 9-16 Fluorescent nanoparticles or quantum dots. Quantum dots are tiny nanoparticles of cadmium selenide, a semiconductor, with a coating to make them water-soluble (A). They can be coupled to protein probes such as antibodies or streptavidin and, when introduced into a cell, will bind to a protein of interest. Different-sized quantum dots emit light of different colors—the larger the dot the longer the wavelength—but they are all excited by the same blue light. (B) Quantum dots can keep shining for weeks, unlike most fluorescent organic dyes. In this cell, a nuclear protein is labeled (green) with an organic fluorescent dye (Alexa 488), while microtubules are stained (red) with quantum dots bound to streptavidin. On continuous exposure to blue light the fluorescent dye fades quickly while the quantum dots continue to fluoresce. (B, from X. Wu et al., *Nat. Biotechnol.* 21:41–46, 2003. With permission from Macmillan Publishers Ltd.)

Antibodies Can Be Used to Detect Specific Molecules

Antibodies are proteins produced by the vertebrate immune system as a defense against infection (discussed in Chapter 24). They are unique among proteins because they are made in billions of different forms, each with a different binding site that recognizes a specific target molecule (or *antigen*). The precise antigen specificity of antibodies makes them powerful tools for the cell biologist. When labeled with fluorescent dyes, antibodies are invaluable for locating specific molecules in cells by fluorescence microscopy (Figure 9-17); labeled with electron-dense particles such as colloidal gold spheres, they are used for similar purposes in the electron microscope (discussed below).

When we use antibodies as probes to detect and assay specific molecules in cells we frequently amplify the fluorescent signal they produce by chemical methods. For example, although a marker molecule such as a fluorescent dye can be linked directly to an antibody used for specific recognition—the *primary antibody*—a stronger signal is achieved by using an unlabeled primary antibody and then detecting it with a group of labeled *secondary antibodies* that bind to it (Figure 9-18). This process is called *indirect immunocytochemistry*.

The most sensitive amplification methods use an enzyme as a marker molecule attached to the secondary antibody. The enzyme alkaline phosphatase, for example, in the presence of appropriate chemicals, produces inorganic phosphate that in turn leads to the local formation of a colored precipitate. This reveals the location of the secondary antibody and hence the location of the antibody–antigen complex. Since each enzyme molecule acts catalytically to generate many thousands of molecules of product, even tiny amounts of antigen can be detected. An enzyme-linked immunosorbent assay (ELISA) based on this principle is frequently used in medicine as a sensitive test—for pregnancy or for various types of infections, for example. Although the enzyme amplification makes enzyme-linked methods very sensitive, diffusion of the colored precipitate away from the enzyme limits the spatial resolution of this method for

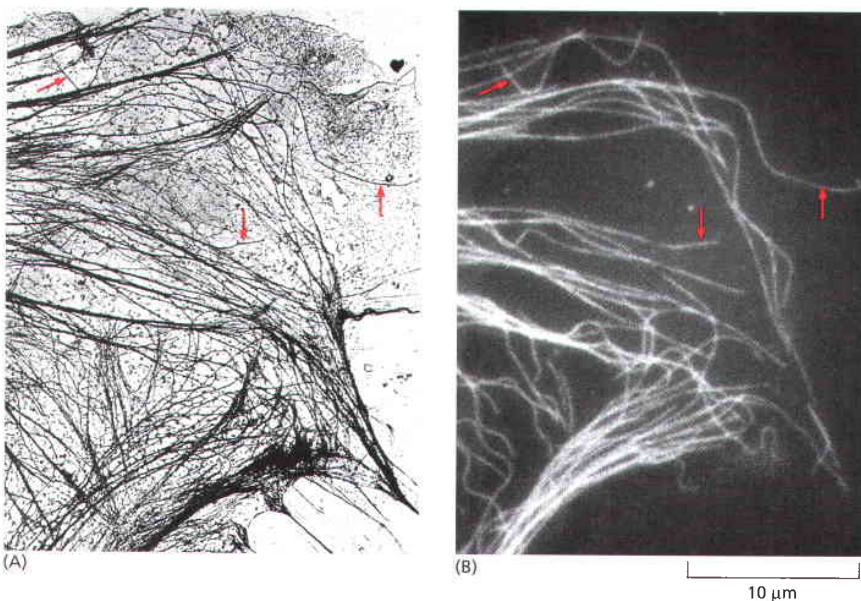


Figure 9-17 Immunofluorescence. (A) A transmission electron micrograph of the periphery of a cultured epithelial cell showing the distribution of microtubules and other filaments. (B) The same area stained with fluorescent antibodies against tubulin, the protein that assembles to form microtubules, using the technique of indirect immunocytochemistry (see Figure 9-18). Red arrows indicate individual microtubules that are readily recognizable in both images. Note that, because of diffraction effects, the microtubules in the light microscope appear 0.2 μm wide rather than their true width of 0.025 μm. (From M. Osborn, R. Webster and K. Weber, *J. Cell Biol.* 77:R27–R34, 1978. With permission from The Rockefeller University Press.)

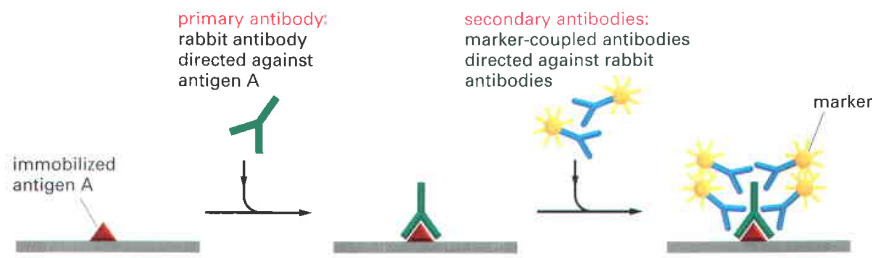


Figure 9–18 Indirect immunocytochemistry. This detection method is very sensitive because many molecules of the secondary antibody recognize each primary antibody. The secondary antibody is covalently coupled to a marker molecule that makes it readily detectable. Commonly used marker molecules include fluorescent dyes (for fluorescence microscopy), the enzyme horseradish peroxidase (for either conventional light microscopy or electron microscopy), colloidal gold spheres (for electron microscopy), and the enzymes alkaline phosphatase or peroxidase (for biochemical detection).

microscopy, and fluorescent labels are usually used for the most precise optical localization.

Antibodies are made most simply by injecting a sample of the antigen several times into an animal such as a rabbit or a goat and then collecting the antibody-rich serum. This *antiserum* contains a heterogeneous mixture of antibodies, each produced by a different antibody-secreting cell (a B lymphocyte). The different antibodies recognize various parts of the antigen molecule (called an antigenic determinant, or epitope), as well as impurities in the antigen preparation. Removing the unwanted antibody molecules that bind to other molecules sharpens the specificity of an antiserum for a particular antigen; an antiserum produced against protein X, for example, when passed through an affinity column of antigens X, will bind to these antigens, allowing other antibodies to pass through the column. Purified anti-X antibody can subsequently be eluted from the column. Even so, the heterogeneity of such antisera sometimes limits their usefulness. The use of monoclonal antibodies largely overcomes this problem (see Figure 8–8). However, monoclonal antibodies can also have problems. Since they are single-antibody protein species, they show almost perfect specificity for a single site or epitope on the antigen, but the accessibility of the epitope, and thus the usefulness of the antibody, may depend on the specimen preparation. For example, some monoclonal antibodies will react only with unfixed antigens, others only after the use of particular fixatives, and still others only with proteins denatured on SDS polyacrylamide gels, and not with the proteins in their native conformation.

Imaging of Complex Three-Dimensional Objects Is Possible with the Optical Microscope

For ordinary light microscopy, as we have seen, a tissue has to be sliced into thin sections to be examined; the thinner the section, the crisper the image. The process of sectioning loses information about the third dimension. How, then, can we get a picture of the three-dimensional architecture of a cell or tissue, and how can we view the microscopic structure of a specimen that, for one reason or another, cannot first be sliced into sections? Although an optical microscope is focused on a particular focal plane within complex three-dimensional specimens, all the other parts of the specimen, above and below the plane of focus, are also illuminated and the light originating from these regions contributes to the image as “out-of-focus” blur. This can make it very hard to interpret the image in detail and can lead to fine image structure being obscured by the out-of-focus light.

Two distinct but complementary approaches solve this problem: one is computational, the other is optical. These three-dimensional microscopic imaging methods make it possible to focus on a chosen plane in a thick specimen while rejecting the light that comes from out-of-focus regions above and below that plane. Thus one sees a crisp, thin *optical section*. From a series of such optical sections taken at different depths and stored in a computer, it is easy to reconstruct a three-dimensional image. The methods do for the microscopist what the CT scanner does (by different means) for the radiologist investigating a human body: both machines give detailed sectional views of the interior of an intact structure.

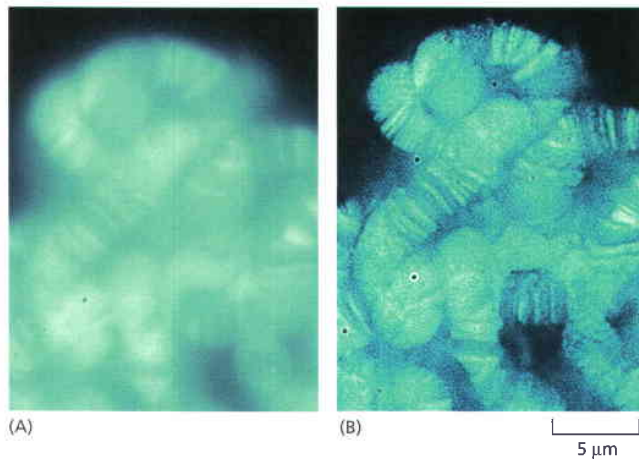


Figure 9-19 Image deconvolution. (A) A light micrograph of the large polytene chromosomes from *Drosophila* stained with a fluorescent DNA-binding dye. (B) The same field of view after image deconvolution clearly reveals the banding pattern on the chromosomes. Each band is about $0.25\ \mu\text{m}$ thick, approaching the resolution limit of the light microscope. (Courtesy of the Joh Sedat Laboratory.)

The computational approach is often called *image deconvolution*. To understand how it works, remember that the wavelike nature of light means that the microscope lens system produces a small blurred disc as the image of a point light source (see Figure 9-5), with increased blurring if the point source lies above or below the focal plane. This blurred image of a point source is called the *point spread function*. An image of a complex object can then be thought of as being built up by replacing each point of the specimen by a corresponding blurred disc, resulting in an image that is blurred overall. For deconvolution, we first obtain a series of (blurred) images, usually with a cooled CCD camera, focusing the microscope in turn on a series of focal planes—in effect, a (blurred) three-dimensional image. The stack of digital images is then processed by computer to remove as much of the blur as possible. Essentially the computer program uses the microscope's point spread function to determine what the effect of the blurring would have been on the image, and then applies an equivalent “deblurring” (deconvolution), turning the blurred three-dimensional image into a series of clean optical sections. The computation required is quite complex, and used to be a serious limitation. However, with faster and cheaper computers, the image deconvolution method is gaining in power and popularity. **Figure 9-19** shows an example.

The Confocal Microscope Produces Optical Sections by Excluding Out-of-Focus Light

The confocal microscope achieves a result similar to that of deconvolution, but does so by manipulating the light before it is measured; thus it is an analog technique rather than a digital one. The optical details of the **confocal microscope** are complex, but the basic idea is simple, as illustrated in **Figure 9-20**, and the results are far superior to those obtained by conventional light microscopy (**Figure 9-21**).

The microscope is generally used with fluorescence optics (see Figure 9-13), but instead of illuminating the whole specimen at once, in the usual way, the optical system at any instant focuses a spot of light onto a single point at a specific depth in the specimen. It requires a very bright source of pinpoint illumination that is usually supplied by a laser whose light has been passed through a pinhole. The fluorescence emitted from the illuminated material is collected and brought to an image at a suitable light detector. A pinhole aperture is placed in front of the detector, at a position that is *confocal* with the illuminating pinhole—that is, precisely where the rays emitted from the illuminated point in the specimen come to a focus. Thus, the light from this point in the specimen converges on this aperture and enters the detector.

By contrast, the light from regions out of the plane of focus of the spotlight is also out of focus at the pinhole aperture and is therefore largely excluded from the detector (see Figure 9-20). To build up a two-dimensional image, data from

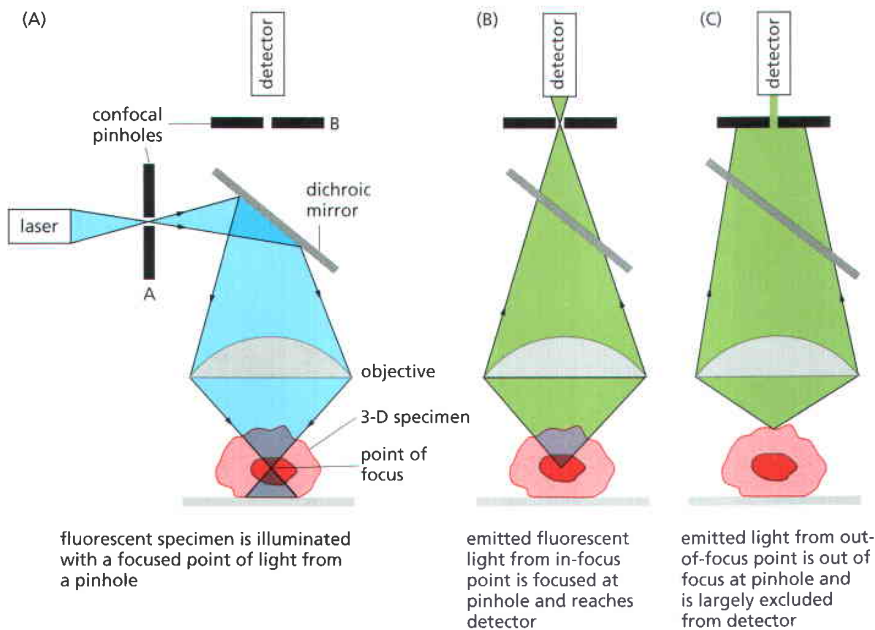


Figure 9-20 The confocal fluorescence microscope. This simplified diagram shows that the basic arrangement of optical components is similar to that of the standard fluorescence microscope shown in Figure 9-13, except that a laser is used to illuminate a small pinhole whose image is focused at a single point in the specimen (A). Emitted fluorescence from this focal point in the specimen is focused at a second (confocal) pinhole (B). Emitted light from elsewhere in the specimen is not focused at the pinhole and therefore does not contribute to the final image (C). By scanning the beam of light across the specimen, a very sharp two-dimensional image of the exact plane of focus is built up that is not significantly degraded by light from other regions of the specimen.

each point in the plane of focus are collected sequentially by scanning across the field in a raster pattern (as on a television screen) and are displayed on a video screen. Although not shown in Figure 9-20, the scanning is usually done by deflecting the beam with an oscillating mirror placed between the dichroic mirror and the objective lens in such a way that the illuminating spotlight and the confocal pinhole at the detector remain strictly in register.

The confocal microscope has been used to resolve the structure of numerous complex three-dimensional objects (Figure 9-22), including the networks of cytoskeletal fibers in the cytoplasm and the arrangements of chromosomes and genes in the nucleus.

The relative merits of deconvolution methods and confocal microscopy for three-dimensional optical microscopy are still the subject of debate. Confocal microscopes are generally easier to use than deconvolution systems and the final optical sections can be seen quickly. In contrast, the cooled CCD (charge-coupled device) cameras used for deconvolution systems are extremely efficient at collecting small amounts of light, and they can be used to make detailed three-dimensional images from specimens that are too weakly stained or too easily damaged by the bright light used for confocal microscopy.

Both methods, however, have another drawback; neither is good at coping with thick specimens. Deconvolution methods quickly become ineffective any deeper than about 40 μm into a specimen, while confocal microscopes can only

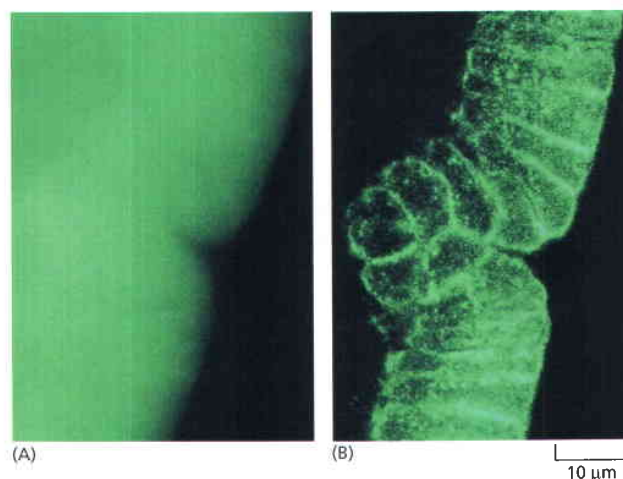


Figure 9-21 Conventional and confocal fluorescence microscopy compared.

These two micrographs are of the same intact gastrula-stage *Drosophila* embryo that has been stained with a fluorescent probe for actin filaments. (A) The conventional, unprocessed image is blurred by the presence of fluorescent structures above and below the plane of focus. (B) In the confocal image, this out-of-focus information is removed, resulting in a crisp optical section of the cells in the embryo. (Courtesy of Richard Warn and Peter Shaw.)

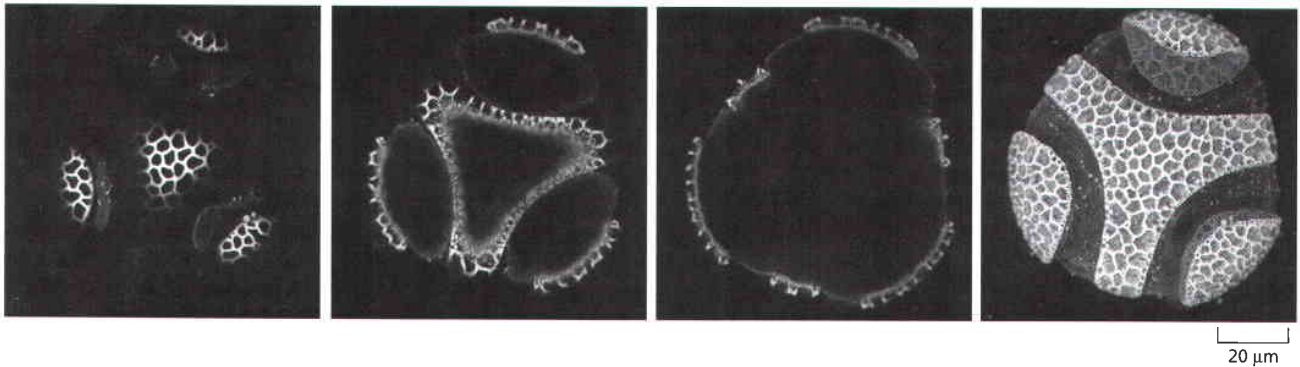


Figure 9–22 Three-dimensional reconstruction from confocal microscope images. Pollen grains, in this case from a passion flower, have a complex sculptured cell wall that contains fluorescent compounds. Images obtained at different depths through the grain, using a confocal microscope, can be recombined to give a three-dimensional view of the whole grain, shown on the right. Three selected individual optical sections from the full set of 30, each of which shows little contribution from its neighbors, are shown on the left. (Courtesy of Brad Amos.)

obtain images up to a depth of about 150 μm . Special confocal microscopes can now take advantage of the way in which fluorescent molecules are excited, to probe even deeper into a specimen. Fluorescent molecules are usually excited by a single high-energy photon, of shorter wavelength than the emitted light, but they can in addition be excited by the absorption of two (or more) photons of lower energy, as long as they both arrive within a femtosecond or so of each other. The use of this longer-wavelength excitation has some important advantages. In addition to reducing background noise, red or near infrared light can penetrate deeper within a specimen. Multiphoton confocal microscopes, constructed to take advantage of this “two-photon” effect, can typically obtain sharp images even at a depth of 0.5 mm within a specimen. This is particularly valuable for studies of living tissues, notably in imaging the dynamic activity of synapses and neurons just below the surface of living brains (**Figure 9–23**).

Fluorescent Proteins Can Be Used to Tag Individual Proteins in Living Cells and Organisms

Even the most stable cellular structures must be assembled, disassembled, and reorganized during the cell’s life cycle. Other structures, often enormous on the molecular scale, rapidly change, move, and reorganize themselves as the cell conducts its internal affairs and responds to its environment. Complex, highly organized pieces of molecular machinery move components around the cell, controlling traffic into and out of the nucleus, from one organelle to another, and into and out of the cell itself.

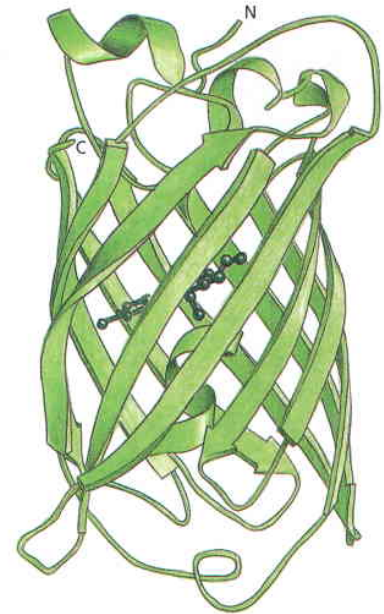
Various techniques have been developed to make specific components of living cells visible in the microscope. Most of these methods use fluorescent proteins, and they require a trade-off between structural preservation and efficient labeling. All of the fluorescent molecules discussed so far are made outside the cell and then artificially introduced into it. Now new opportunities have been opened up by the discovery of genes coding for protein molecules that are themselves inherently fluorescent. Genetic engineering then enables the creation of lines of cells or organisms that make their own visible tags and labels, without the introduction of foreign molecules. These cellular exhibitionists display their inner workings in glowing fluorescent color.

Foremost among the fluorescent proteins used for these purposes by cell biologists is the **green fluorescent protein (GFP)**, isolated from the jellyfish *Aequoria victoria*. This protein is encoded in the normal way by a single gene that can be cloned and introduced into cells of other species. The freshly translated protein is not fluorescent, but within an hour or so (less for some alleles of



Figure 9–23 Multi-photon imaging. Infrared laser light causes less damage to living cells and can also penetrate further, allowing microscopists to peer deeper into living tissues. The two-photon effect, in which a fluorochrome can be excited by two coincident infrared photons instead of a single high-energy photon, allows us to see nearly 0.5 mm inside the cortex of a live mouse brain. A dye, whose fluorescence changes with the calcium concentration, reveals active synapses (yellow) on the dendritic spines (red) that change as a function of time. (Courtesy of Karel Svoboda.)

Figure 9–24 Green fluorescent protein (GFP). The structure of GFP, shown here schematically, highlights the eleven β strands that form the staves of a barrel. Buried within the barrel is the active chromophore (dark green) that is formed post-translationally from the protruding side chains of three amino acid residues. (Adapted from M. Ormö et al., *Science* 273:1392–1395, 1996. With permission from AAAS.)



the gene, more for others) it undergoes a self-catalyzed post-translational modification to generate an efficient and bright fluorescent center, shielded within the interior of a barrel-like protein (Figure 9–24). Extensive site-directed mutagenesis performed on the original gene sequence has resulted in useful fluorescence in organisms ranging from animals and plants to fungi and microbes. The fluorescence efficiency has also been improved, and variants have been generated with altered absorption and emission spectra in the blue–green–yellow range. Recently a family of related fluorescent proteins discovered in corals, has extended the range into the red region of the spectrum (see Figure 9–14).

One of the simplest uses of GFP is as a reporter molecule, a fluorescent probe to monitor gene expression. A transgenic organism can be made with the GFP-coding sequence placed under the transcriptional control of the promoter belonging to a gene of interest, giving a directly visible readout of the gene's expression pattern in the living organism (Figure 9–25). In another application, a peptide location signal can be added to the GFP to direct it to a particular cellular compartment, such as the endoplasmic reticulum or a mitochondrion, lighting up these organelles so they can be observed in the living state (see Figure 12–35B).

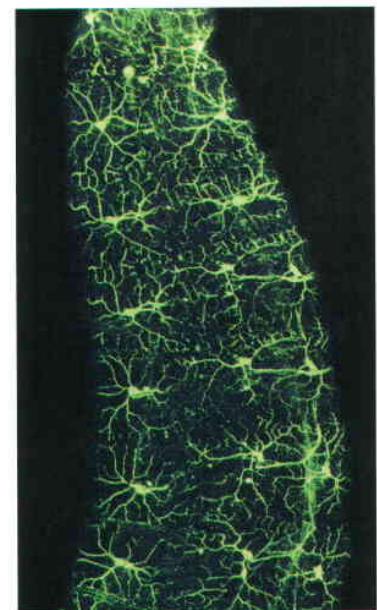
The GFP DNA-coding sequence can also be inserted at the beginning or end of the gene for another protein, yielding a chimeric product consisting of that protein with a GFP domain attached. In many cases, this GFP-fusion protein behaves in the same way as the original protein, directly revealing its location and activities by means of its genetically encoded contrast (Figure 9–26). <TAAT> It is often possible to prove that the GFP-fusion protein is functionally equivalent to the untagged protein, for example by using it to rescue a mutant lacking that protein. GFP tagging is the clearest and most unequivocal way of showing the distribution and dynamics of a protein in a living organism (Figure 9–27). <TTCT>

Protein Dynamics Can Be Followed in Living Cells

Fluorescent proteins are now exploited, not just to see where in a cell a particular protein is located, but also to uncover its kinetic properties and to find out whether it might interact with other proteins. We now describe three techniques in which GFP and its relatives are used in this way.

The first is the monitoring of interactions between one protein and another by **fluorescence resonance energy transfer (FRET)**. In this technique, whose principles have been described earlier (see Figure 8–26), the two molecules of interest are each labeled with a different fluorochrome, chosen so that the emission spectrum of one fluorochrome overlaps with the absorption spectrum of the other. If the two proteins bind so as to bring their fluorochromes into very close proximity (closer than about 5 nm), one fluorochrome transfers the energy of the absorbed light directly to the other. Thus, when the complex is illuminated at the excitation wavelength of the first fluorochrome, fluorescent light is pro-

Figure 9–25 Green fluorescent protein (GFP) as a reporter. For this experiment, carried out in the fruit fly, the GFP gene was joined (using recombinant DNA techniques) to a fly promoter that is active only in a specialized set of neurons. This image of a live fly embryo was captured by a fluorescence microscope and shows approximately 20 neurons, each with long projections (axons and dendrites) that communicate with other (nonfluorescent) cells. These neurons are located just under the surface of the animal and allow it to sense its immediate environment. (From W.B. Grueber et al., *Curr. Biol.* 13:618–626, 2003. With permission from Elsevier.)



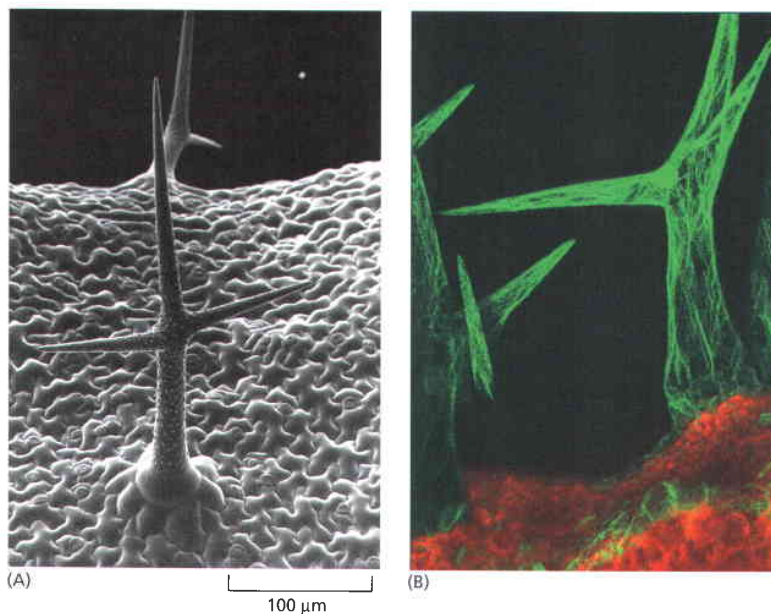


Figure 9-26 GFP-tagged proteins.

(A) The upper surface of the leaves of *Arabidopsis* plants are covered with huge branched single-cell hairs that rise up from the surface of the epidermis. These hairs, or trichomes, can be imaged in the scanning electron microscope. (B) If an *Arabidopsis* plant is transformed with a DNA sequence coding for talin (an actin-binding protein), fused to a DNA sequence coding for GFP, the fluorescent talin protein produced binds to actin filaments in all the living cells of the transgenic plant. Confocal microscopy can reveal the dynamics of the entire actin cytoskeleton of the trichome (*green*). The red fluorescence arises from chlorophyll in cells within the leaf below the epidermis. (A, courtesy of Paul Linstead; B, courtesy of Jaideep Mathur.)

duced at the emission wavelength of the second. This method can be used with two different spectral variants of GFP as fluorochromes to monitor processes such as the interaction of signaling molecules with their receptors, or proteins in macromolecular complexes (Figure 9-28).

The complexity and rapidity of many intracellular processes, such as the actions of signaling molecules or the movements of cytoskeletal proteins, make them difficult to study at a single-cell level. Ideally, we would like to be able to introduce any molecule of interest into a living cell at a precise time and location and follow its subsequent behavior, as well as the response of the cell to that molecule. Microinjection is limited by the difficulty of controlling the place and time of delivery. A more powerful approach involves synthesizing an inactive form of the fluorescent molecule of interest, introducing it into the cell, and then activating it suddenly at a chosen site in the cell by focusing a spot of light on it. This process is referred to as **photoactivation**. Inactive photosensitive precursors of this type, often called *caged molecules*, have been made for many fluorescent molecules. A microscope can be used to focus a strong pulse of light from a laser on any tiny region of the cell, so that the experimenter can control exactly where and when the fluorescent molecule is photoactivated.

One class of caged fluorescent proteins is made by attaching a photoactivatable fluorescent tag to a purified protein. It is important that the modified protein remain biologically active: labeling with a caged fluorescent dye adds a bulky group to the surface of a protein, which can easily change the protein's properties. A satisfactory labeling protocol is usually found by trial and error. Once a biologically active labeled protein has been produced, it needs to be introduced into the living cell (see Figure 9-34), where its behavior can be followed. Tubulin, labeled with caged fluorescein for example, when injected into a dividing cell, can be incorporated into microtubules of the mitotic spindle.

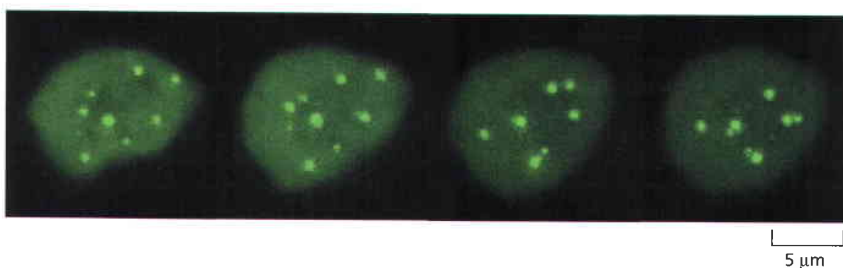


Figure 9-27 Dynamics of GFP tagging.

This sequence of micrographs shows a set of three-dimensional images of a living nucleus taken over the course of an hour. Tobacco cells have been stably transformed with GFP fused to a spliceosomal protein that is concentrated in small nuclear bodies called Cajal bodies (see Figure 6-48). The fluorescent Cajal bodies, easily visible in a living cell with confocal microscopy, are dynamic structures that move around within the nucleus. (Courtesy of Kurt Boudonck, Liam Dolan, and Peter Shaw.)

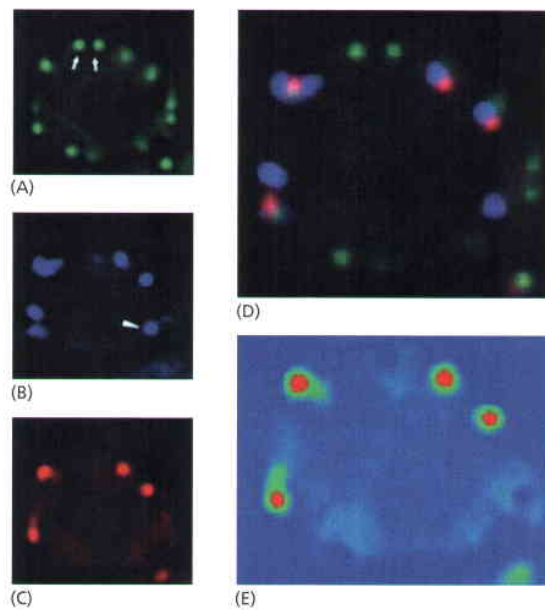


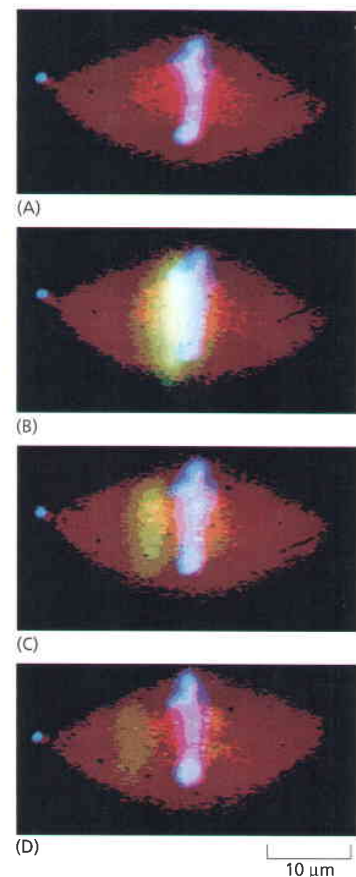
Figure 9–28 Fluorescence resonance energy transfer (FRET) imaging. This experiment shows that a protein called Sla1p can interact tightly with another protein, called Abp1p, which is involved in cortical actin attachment at the surface of a budding yeast cell. Sla1p is expressed in the yeast cell (A) as a fusion protein with a yellow variant of GFP (YFP), while Abp1p is expressed as a fusion protein (B) with a cyan variant of GFP (CFP). The FRET signal (see also Figure 8–26), displayed here in red (C), is obtained by exciting the CFP but recording only the fluorescence emitted from the YFP, which will occur only when the two molecules are tightly associated (within 0.5 nm). The spots at the cortex (D), seen when (A), (B), and (C) are superimposed, are of three sorts, those where Sla1p is found alone (arrows in A), those where Abp1p is found alone (arrowhead in B), and those where they are closely associated and generate a FRET signal, shown in the false-colored and corrected image (E). Since Sla1p was already known to form part of the endocytic machinery, this experiment physically connects that process with the process of actin attachment to the cell cortex. (From D.T. Warren et al., *J. Cell Sci.* 115:1703–1715, 2002. With permission from The Company of Biologists.)

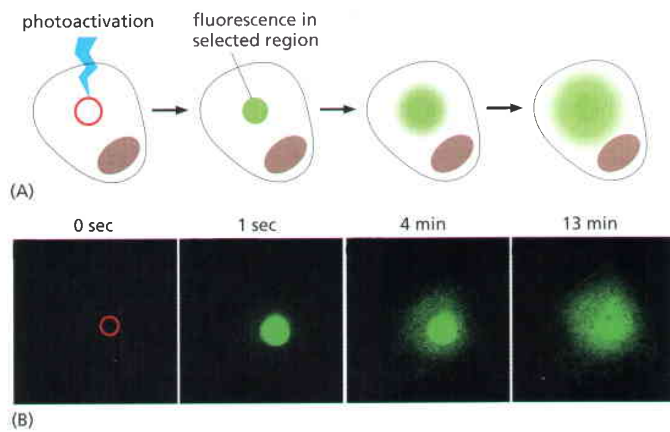
When a small region of the spindle is illuminated with a laser, the labeled tubulin becomes fluorescent, so that its movement along the spindle microtubules can be readily followed (Figure 9–29).

A more recent development in photoactivation is the discovery that the genes encoding GFP and related fluorescent proteins can be mutated to produce protein variants, usually with a single amino acid change, that fluoresce only weakly under normal excitation conditions, but can be induced to fluoresce strongly by activating them with a strong pulse of light at a different wavelength. In principle the microscopist can then follow the local *in vivo* behavior of any protein that can be expressed as a fusion with one of these GFP variants. These genetically encoded, photoactivatable fluorescent proteins thus avoid the need to introduce the probe into the cell, and allow the lifetime and behaviour of any protein to be studied independently of other newly synthesized proteins (Figure 9–30).

A third way to exploit GFP fused to a protein of interest is to use a strong focussed beam of light from a laser to extinguish the GFP fluorescence in a specified region of the cell. By analyzing the way in which the remaining fluorescent protein molecules move into the bleached area as a function of time, we can obtain information about the protein's kinetic parameters. This technique, usually carried out with a confocal microscope, is known as **fluorescence recovery after photobleaching (FRAP)** and, like photoactivation, can deliver valuable quantitative data about the protein of interest, such as diffusion coefficients <ATGT>, active transport rates, or binding and dissociation rates from other proteins (Figure 9–31).

Figure 9–29 Determining microtubule flux in the mitotic spindle with caged fluorescein linked to tubulin. (A) A metaphase spindle formed *in vitro* from an extract of *Xenopus* eggs has incorporated three fluorescent markers: rhodamine-labeled tubulin (red) to mark all the microtubules, a blue DNA-binding dye that labels the chromosomes, and caged-fluorescein-labeled tubulin, which is also incorporated into all the microtubules but is invisible because it is nonfluorescent until activated by ultraviolet light. (B) A beam of UV light uncages the caged-fluorescein-labeled tubulin locally, mainly just to the left side of the metaphase plate. Over the next few minutes (after 1.5 minutes in C, after 2.5 minutes in D), the uncaged-fluorescein–tubulin signal moves toward the left spindle pole, indicating that tubulin is continuously moving poleward even though the spindle (visualized by the red rhodamine-labeled tubulin fluorescence) remains largely unchanged. (From K.E. Sawin and T.J. Mitchison, *J. Cell Biol.* 112:941–954, 1991. With permission from The Rockefeller University Press.)





Light-Emitting Indicators Can Measure Rapidly Changing Intracellular Ion Concentrations

One way to study the chemistry of a single living cell is to insert the tip of a fine, glass, ion-sensitive **microelectrode** directly into the cell interior through the plasma membrane. This technique is used to measure the intracellular concentrations of common inorganic ions, such as H^+ , Na^+ , K^+ , Cl^- , and Ca^{2+} . However, ion-sensitive microelectrodes reveal the ion concentration only at one point in a cell, and for an ion present at a very low concentration, such as Ca^{2+} , their responses are slow and somewhat erratic. Thus, these microelectrodes are not ideally suited to record the rapid and transient changes in the concentration of cytosolic Ca^{2+} that have an important role in allowing cells to respond to extracellular signals. Such changes can be analyzed with **ion-sensitive indicators**, whose light emission reflects the local concentration of the ion. Some of these indicators are luminescent (emitting light spontaneously), while others are fluorescent (emitting light on exposure to light).

Aequorin is a luminescent protein isolated from a marine jellyfish; it emits light in the presence of Ca^{2+} and responds to changes in Ca^{2+} concentration in the range of $0.5\text{--}10\ \mu\text{M}$. If microinjected into an egg, for example, aequorin emits a flash of light in response to the sudden localized release of free Ca^{2+} into the cytoplasm that occurs when the egg is fertilized (Figure 9-32). Aequorin has also been expressed transgenically in plants and other organisms to provide a method of monitoring Ca^{2+} in all their cells without the need for microinjection, which can be a difficult procedure.

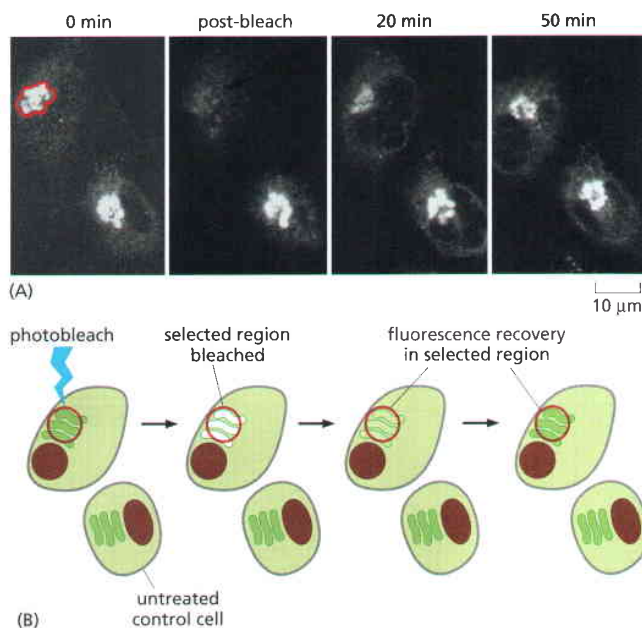


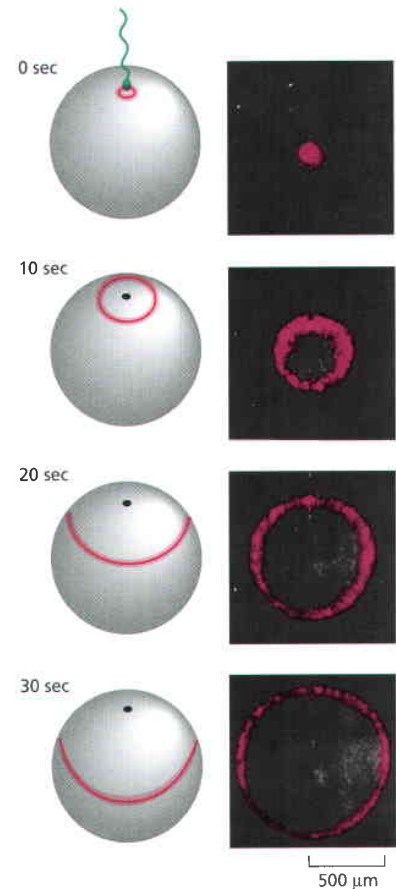
Figure 9-30 Photoactivation.

Photoactivation is the light-induced activation of an inert molecule to an active state. In this experiment a photoactivatable variant of GFP is expressed in a cultured animal cell. Before activation (time 0), little or no GFP fluorescence is detected in the selected region (red circle) when excited by blue light at 488 nm. After activation of the GFP however, using a UV laser pulse at 413 nm, it rapidly fluoresces brightly in the selected region (green). The movement of GFP, as it diffuses out of this region, can be measured. Since only the photoactivated proteins are fluorescent within the cell, the trafficking, turnover and degradative pathways of proteins can be monitored. (B, from J. Lippincott-Schwartz and G.H. Patterson, *Science* 300:87–91, 2003. With permission from AAAS.)

Figure 9-31 Fluorescence recovery after photobleaching (FRAP).

A strong focused pulse of laser light will extinguish, or bleach, the fluorescence of GFP. By selectively photobleaching a set of fluorescently tagged protein molecules within a defined region of a cell, the microscopist can monitor recovery over time, as the remaining fluorescent molecules move into the bleached region. The experiment shown in (A) uses monkey cells in culture that express galactosyltransferase, an enzyme that constantly recycles between the Golgi apparatus and the endoplasmic reticulum. The Golgi apparatus in one of the two cells is selectively photobleached, while the production of new fluorescent protein is blocked by treating the cells with cycloheximide. The recovery, resulting from fluorescent enzyme molecules moving from the ER to the Golgi, can then be followed over a period of time. (B) Schematic diagram of the experiment shown in (A). (A, from J. Lippincott-Schwartz et al., *Histochem. Cell Biol.* 116:97–107, 2001. With permission from Springer-Verlag.)

Figure 9–32 Aequorin, a luminescent protein. The luminescent protein aequorin emits light in the presence of free Ca^{2+} . Here, an egg of the medaka fish has been injected with aequorin, which has diffused throughout the cytosol, and the egg has then been fertilized with a sperm and examined with the help of a very sensitive camera. The four photographs were taken looking down on the site of sperm entry at intervals of 10 seconds and reveal a wave of release of free Ca^{2+} into the cytosol from internal stores just beneath the plasma membrane. This wave sweeps across the egg starting from the site of sperm entry, as indicated in the diagrams on the left. (Photographs reproduced from J.C. Gilkey, L.F. Jaffe, E.B. Ridgway and G.T. Reynolds, *J. Cell Biol.* 76:448–466, 1978. With permission from The Rockefeller University Press.)



Bioluminescent molecules like aequorin emit tiny amounts of light—at best, a few photons per indicator molecule—that are difficult to measure. Fluorescent indicators produce orders of magnitude more photons per molecule; they are therefore easier to measure and can give better spatial resolution. Fluorescent Ca^{2+} indicators have been synthesized that bind Ca^{2+} tightly and are excited by or emit light at slightly different wavelengths when they are free of Ca^{2+} than when they are in their Ca^{2+} -bound form. By measuring the ratio of fluorescence intensity at two excitation or emission wavelengths, we can determine the concentration ratio of the Ca^{2+} -bound indicator to the Ca^{2+} -free indicator, thereby providing an accurate measurement of the free Ca^{2+} concentration. **<CGTC>** Indicators of this type are widely used for second-by-second monitoring of changes in intracellular Ca^{2+} concentrations in the different parts of a cell viewed in a fluorescence microscope (**Figure 9–33**). **<AGGA>**

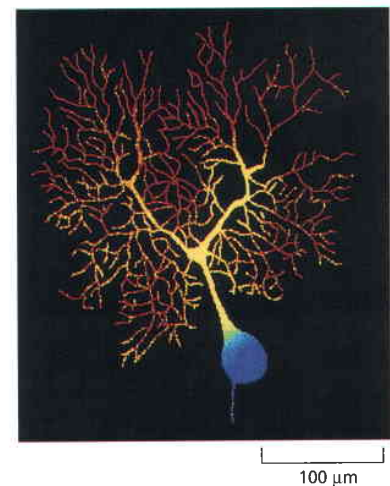
Similar fluorescent indicators measure other ions; some detect H^+ , for example, and hence measure intracellular pH. Some of these indicators can enter cells by diffusion and thus need not be microinjected; this makes it possible to monitor large numbers of individual cells simultaneously in a fluorescence microscope. New types of indicators, used in conjunction with modern image-processing methods, are leading to similarly rapid and precise methods for analyzing changes in the concentrations of many types of small molecules in cells.

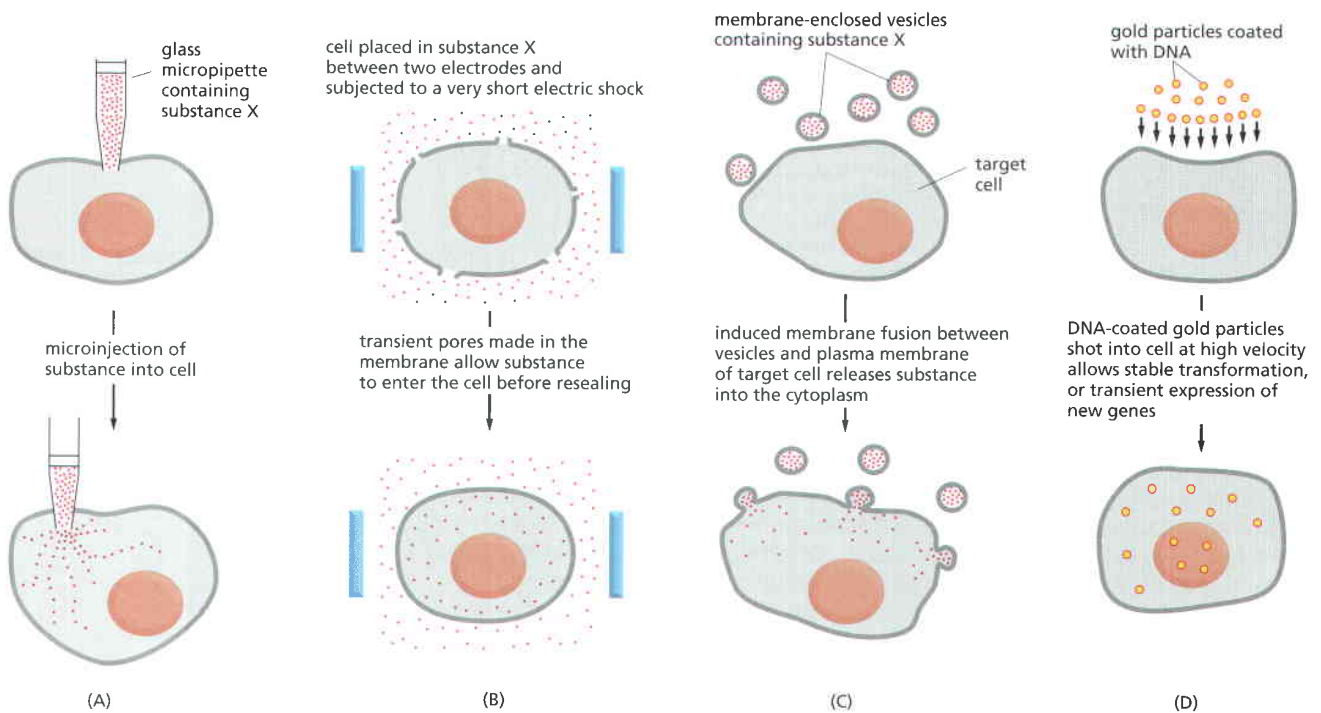
Several Strategies Are Available by Which Membrane-Impermeant Substances Can Be Introduced into Cells

It is often useful to introduce membrane-impermeant molecules into a living cell, whether they are antibodies that recognize intracellular proteins, normal cell proteins tagged with a fluorescent label, or molecules that influence cell behavior. One approach is to microinject the molecules into the cell through a glass micropipette.

When microinjected into a cell, antibodies can block the function of the molecule that they recognize. Anti-myosin-II antibodies injected into a fertilized sea urchin egg, for example, prevent the egg cell from dividing in two, even though nuclear division occurs normally. This observation demonstrates that this myosin has an essential role in the contractile process that divides the cytoplasm during cell division, but that it is not required for nuclear division.

Figure 9–33 Visualizing intracellular Ca^{2+} concentrations by using a fluorescent indicator. The branching tree of dendrites of a Purkinje cell in the cerebellum receives more than 100,000 synapses from other neurons. The output from the cell is conveyed along the single axon seen leaving the cell body at the bottom of the picture. This image of the intracellular Ca^{2+} concentration in a single Purkinje cell (from the brain of a guinea pig) was taken with a low-light camera and the Ca^{2+} -sensitive fluorescent indicator fura-2. The concentration of free Ca^{2+} is represented by different colors, *red* being the highest and *blue* the lowest. The highest Ca^{2+} levels are present in the thousands of dendritic branches. (Courtesy of D.W. Tank, J.A. Connor, M. Sugimori and R.R. Llinas.)





Microinjection, although widely used, demands that each cell be injected individually; therefore, it is possible to study at most only a few hundred cells at a time. Other approaches allow large populations of cells to be permeabilized simultaneously. Partly disrupting the structure of the cell plasma membrane, for example, makes it more permeable; this is usually accomplished by using a powerful electric shock or a chemical such as a low concentration of detergent. The electrical technique has the advantage of creating large pores in the plasma membrane without damaging intracellular membranes. Depending on the cell type and the size of the electric shock, the pores allow even macromolecules to enter (and leave) the cytosol rapidly. This process of *electroporation* is valuable also in molecular genetics, as a way of introducing DNA molecules into cells. With a limited treatment, a large fraction of the cells repair their plasma membrane and survive.

A third method for introducing large molecules into cells is to cause membrane-enclosed vesicles that contain these molecules to fuse with the cell's plasma membrane thus delivering their cargo. This method is used routinely to deliver nucleic acids into mammalian cells, either DNA for transfection studies or RNA for RNAi experiments (discussed in Chapter 8). In the medical field it is also being explored as a method for the targeted delivering of new pharmaceuticals.

Finally, DNA and RNA can also be physically introduced into cells by simply blasting them in at high velocity, coated onto tiny gold particles. Living cells, shot with these nucleic-acid-coated gold particles (typically less than $1\ \mu\text{m}$ in diameter) can successfully incorporate the introduced RNA (used for transient expression studies or RNAi, for example) or DNA (for stable transfection). All four of these methods, illustrated in **Figure 9-34**, are used widely in cell biology.

Figure 9-34 Methods of introducing a membrane-impermeant substance into a cell. (A) The substance is injected through a micropipette, either by applying pressure or, if the substance is electrically charged, by applying a voltage that drives the substance into the cell as an ionic current (a technique called *iontophoresis*). (B) The cell membrane is made transiently permeable to the substance by disrupting the membrane structure with a brief but intense electric shock (2000 V/cm for 200 μsec , for example). (C) Membrane-enclosed vesicles are loaded with the desired substance and then induced to fuse with the target cells. (D) Gold particles coated with DNA are used to introduce a novel gene into the nucleus.

Light Can Be Used to Manipulate Microscopic Objects As Well As to Image Them

Photons carry a small amount of momentum. This means that an object that absorbs or deflects a beam of light experiences a small force. With ordinary light sources, this radiation pressure is too small to be significant. But it is important on a cosmic scale (helping prevent gravitational collapse inside stars), and, more

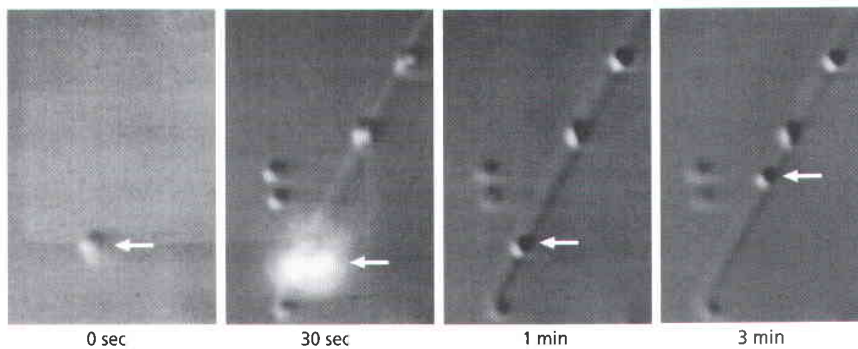


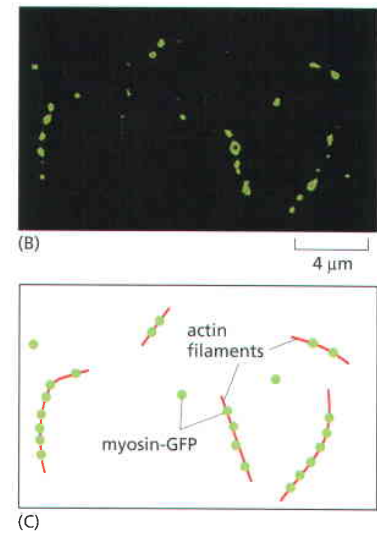
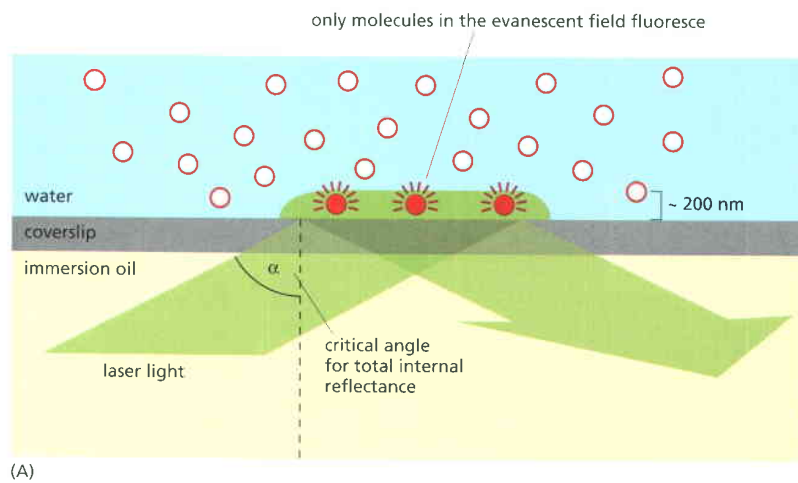
Figure 9–35 Optical tweezers. A focused laser beam can be used to trap microscopic particles and move them about at will. <CGCG> In this experiment, such optical tweezers are used to pick up a small silica bead (0.2 μm , arrow), coated with few kinesin molecules (0 sec), and place it on an isolated ciliary axoneme that is built from microtubules (30 sec). The bright halo seen here is the reflection of the laser at the interface between the water and the coverslip. The kinesin on the released bead (1 min) couples ATP hydrolysis to movement along the microtubules of the axoneme, and powers the transport of the bead along it (3 min). (From S.M. Block et al., *Nature* 348:348–352, 1990. With permission from Macmillan Publishers Ltd.)

modestly, in the cell biology lab, where an intense focused laser beam can exert large enough forces to push small objects around inside a cell. If the laser beam is focused on an object having a higher refractive index than its surroundings, the beam is refracted, causing very large numbers of photons to change direction. The pattern of photon deflection holds the object at the focus of the beam; if it begins to drift away from this position, radiation pressure pushes it back by acting more strongly on one side than the other. Thus, by steering a focused laser beam, usually an infrared laser, which is minimally absorbed by the cellular constituents, one can create “**optical tweezers**” to move subcellular objects like organelles and chromosomes around. This method, sometimes referred to as laser tweezers <CGCG> <CACA>, has been used to measure the forces exerted by single actin–myosin molecules, by single microtubule motors, and by RNA polymerase (Figure 9–35).

Intense focused laser beams that are more strongly absorbed by biological material can also be used more straightforwardly as optical knives—to kill individual cells, to cut or burn holes in them, or to detach one intracellular component from another. In these ways, optical devices can provide a basic toolkit for cellular microsurgery.

Single Molecules Can Be Visualized by Using Total Internal Reflection Fluorescence Microscopy

While beads can be used as markers to track protein movements, it is clearly preferable to be able to visualize the proteins themselves. In principle this can be accomplished by labeling the protein with a fluorescent molecule, either by chemically attaching a small fluorescent molecule to isolated protein molecules or by expressing fluorescent protein fusion constructs (see p. 593). In ordinary microscopes, however, single fluorescent molecules cannot be reliably detected. The limitation has nothing to do with the resolution limit, but instead arises from the interference of light emitted by out-of-focus molecules that tends to blot out the fluorescence from the particular molecule of interest. This problem can be solved by the use of a specialized optical technique called total internal reflectance fluorescence (TIRF) microscopy. In a TIRF microscope, laser light shines onto the coverslip surface at the precise critical angle at which total internal reflection occurs (Figure 9–36A). Because of total internal reflection, the light does not enter the sample, and the majority of fluorescent molecules are not, therefore, illuminated. However, electromagnetic energy does extend, as an evanescent field, for a very short distance beyond the surface of the coverslip and into the specimen, allowing just those molecules in the layer closest to the surface to become excited. When these molecules fluoresce, their emitted light is no longer competing with out-of-focus light from the overlying molecules, and can now be detected. TIRF has allowed several dramatic experiments, for instance imaging of single motor proteins moving along microtubules or single actin filaments forming and branching, although at present the technique is restricted to a thin layer within only 100–200 nm of the cell surface (Figure 9–36B and C).



Individual Molecules Can Be Touched and Moved Using Atomic Force Microscopy

While TIRF allows single molecules to be visualized, it is strictly a passive observation method. In order to probe molecular function, it is ultimately useful to be able to manipulate individual molecules themselves, and atomic force microscopy (AFM) provides a method to do just that. In an AFM device, an extremely small and sharply pointed tip, of silicon or silicon nitride, is made using nanofabrication methods similar to those used in the semiconductor industry. The tip of the AFM is attached to a springy cantilever arm mounted on a highly precise positioning system that allows it to be moved over very small distances. In addition to this precise movement capability, the AFM is able to measure the mechanical force felt by its tip as it moves over the surface (**Figure 9–37A**). When AFM was first developed, it was intended as an imaging technology to measure molecular-scale features on a surface. When used in this mode, the probe is scanned over the surface, moving up and down as necessary to maintain a constant interaction force with the surface, thus revealing any objects such as proteins that might be present on the otherwise flat surface (see **Figures 10–14** and **10–32**). AFM is not limited to simply imaging surfaces, however, and can also be used to pick up and move single molecules, in a molecular-scale version of the optical tweezers described above. Using this technology, the mechanical properties of individual protein molecules can be measured in detail. For example, AFM has been used to unfold a single protein molecule in order to measure the energetics of domain folding (**Figure 9–37B**). The full potential to probe proteins mechanically, as well as to assemble individual proteins into defined arrangements using AFM, is only now starting to be explored, but it seems likely that this tool will become increasingly important in the future.

Molecules Can Be Labeled with Radioisotopes

As we have just seen, in cell biology it is often important to determine the quantities of specific molecules and to know where they are in the cell and how their level or location changes in response to extracellular signals. The molecules of interest range from small inorganic ions, such as Ca^{2+} or H^+ , to large macromolecules, such as specific proteins, RNAs, or DNA sequences. We have so far described how sensitive fluorescence methods can be used for assaying these types of molecules, as well as for following the dynamic behavior of many of them in living cells. In ending this section, we describe how radioisotopes are used to trace the path of specific molecules through the cell.

Figure 9–36 TIRF microscopy allows the detection of single fluorescent molecules. (A) TIRF microscopy uses excitatory laser light to illuminate the coverslip surface at the critical angle at which all the light is reflected by the glass–water interface. Some electromagnetic energy extends a short distance across the interface as an evanescent wave that excites just those molecules that are very close to the surface. (B) TIRF microscopy is used here to image individual myosin-GFP molecules (green dots) attached to non-fluorescent actin filaments (C), which are invisible but stuck to the surface of the coverslip. (Courtesy of Dmitry Cherny and Clive R. Bagshaw.)

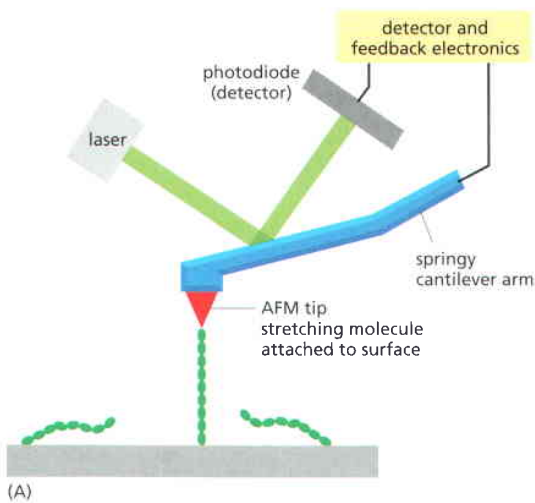
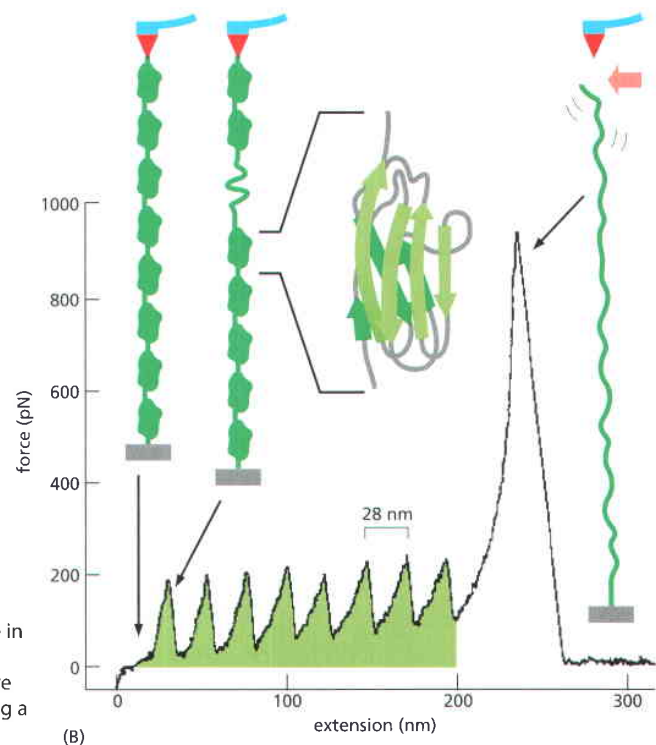


Figure 9–37 Single protein molecules can be manipulated by atomic force microscopy. (A) Schematic diagram of the key components of an atomic force microscope (AFM), showing the force-sensing tip attached to one end of a single protein molecule in the experiment described in (B). (B) Titin is an enormous protein molecule that provides muscle with its passive elasticity (see Figure 16–76). The extensibility of this protein can be tested directly, using a short artificially produced protein that contains eight repeated Ig-domains from one region of the titin protein. In this experiment the tip of the AFM is used to pick up, and progressively stretch, a single molecule until it eventually ruptures. As force is applied, each Ig-domain suddenly begins to unfold, and the force needed in each case (about 200 pN) can be recorded. The region of the force–extension curve shown in green records the sequential unfolding event for each of the eight protein domains. (Adapted from W.A. Linke et al., *J. Struct. Biol.* 137:194–205, 2002. With permission from Elsevier.)



Most naturally occurring elements are a mixture of slightly different isotopes. These differ from one another in the mass of their atomic nuclei, but because they have the same number of protons and electrons, they have the same chemical properties. In radioactive isotopes, or radioisotopes, the nucleus is unstable and undergoes random disintegration to produce a different atom. In the course of these disintegrations, either energetic subatomic particles, such as electrons, or radiations, such as gamma-rays, are given off. By using chemical synthesis to incorporate one or more radioactive atoms into a small molecule of interest, such as a sugar or an amino acid, the fate of that molecule (and of specific atoms in it) can be traced during any biological reaction.

Although naturally occurring radioisotopes are rare (because of their instability), they can be produced in large amounts in nuclear reactors, where stable atoms are bombarded with high-energy particles. As a result, radioisotopes of many biologically important elements are readily available (Table 9–1). The radiation they emit is detected in various ways. Electrons (β particles) can be detected in a Geiger counter by the ionization they produce in a gas, or they can be measured in a scintillation counter by the small flashes of light they induce in a scintillation fluid. These methods make it possible to measure accurately the quantity of a particular radioisotope present in a biological specimen. Using either light or electron microscopy, it is also possible to determine the location of a radioisotope in a specimen by autoradiography, as we describe below. All of these methods of detection are extremely sensitive: in favorable circumstances, nearly every disintegration—and therefore every radioactive atom that decays—can be detected.

Table 9–1 Some Radioisotopes in Common Use in Biological Research

ISOTOPE	HALF-LIFE
^{32}P	14 days
^{131}I	8.1 days
^{35}S	87 days
^{14}C	5570 years
^{45}Ca	164 days
^3H	12.3 years

The isotopes are arranged in decreasing order of the energy of the β radiation (electrons) they emit. ^{131}I also emits γ radiation. The half-life is the time required for 50% of the atoms of an isotope to disintegrate.

Radioisotopes Are Used to Trace Molecules in Cells and Organisms

One of the earliest uses of radioactivity in biology was to trace the chemical pathway of carbon during photosynthesis. Unicellular green algae were maintained in an atmosphere containing radioactively labeled CO_2 ($^{14}\text{CO}_2$), and at various times after they had been exposed to sunlight, their soluble contents were separated by paper chromatography. Small molecules containing ^{14}C atoms derived from CO_2 were detected by a sheet of photographic film placed over the dried paper chromatogram. In this way most of the principal components in the photosynthetic pathway from CO_2 to sugar were identified.

Radioactive molecules can be used to follow the course of almost any process in cells. In a typical experiment the cells are supplied with a precursor molecule in radioactive form. The radioactive molecules mix with the preexisting unlabeled ones; both are treated identically by the cell as they differ only in the weight of their atomic nuclei. Changes in the location or chemical form of the radioactive molecules can be followed as a function of time. The resolution of such experiments is often sharpened by using a pulse-chase labeling protocol, in which the radioactive material (the pulse) is added for only a very brief period and then washed away and replaced by nonradioactive molecules (the chase). Samples are taken at regular intervals, and the chemical form or location of the radioactivity is identified for each sample (Figure 9–38). Pulse-chase experiments, combined with autoradiography, have been important, for example, in elucidating the pathway taken by secreted proteins from the ER to the cell exterior.

Radioisotopic labeling is a uniquely valuable way of distinguishing between molecules that are chemically identical but have different histories—for example, those that differ in their time of synthesis. In this way, for example, it was shown that almost all of the molecules in a living cell are continually being degraded and replaced, even when the cell is not growing and is apparently in a steady state. This “turnover,” which sometimes takes place very slowly, would be almost impossible to detect without radioisotopes.

Today, nearly all common small molecules are available in radioactive form from commercial sources, and virtually any biological molecule, no matter how complicated, can be radioactively labeled. Compounds can be made with radioactive atoms incorporated at particular positions in their structure, enabling the separate fates of different parts of the same molecule to be followed during biological reactions (Figure 9–39).

As mentioned previously, one of the important uses of radioactivity in cell biology is to localize a radioactive compound in sections of whole cells or tissues by autoradiography. In this procedure, living cells are briefly exposed to a pulse of a specific radioactive compound and then incubated for a variable period—to allow them time to incorporate the compound—before being fixed and processed for light or electron microscopy. Each preparation is then overlaid with a thin film of photographic emulsion and left in the dark for several days, during which the radioisotope decays. The emulsion is then developed, and the position of the radioactivity in each cell is indicated by the position of the developed silver grains (see Figure 5–29). If cells are exposed to ^3H -thymidine, a radioactive precursor of DNA, for example, it can be shown that DNA is made in the nucleus

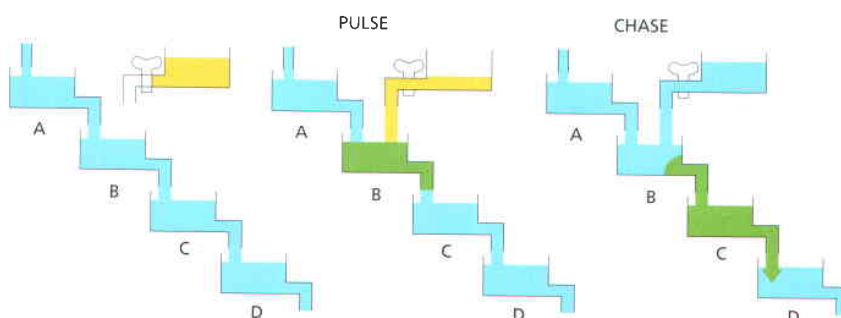


Figure 9–38 The logic of a typical pulse-chase experiment using radioisotopes. The chambers labeled A, B, C, and D represent either different compartments in the cell (detected by autoradiography or by cell-fractionation experiments) or different chemical compounds (detected by chromatography or other chemical methods).

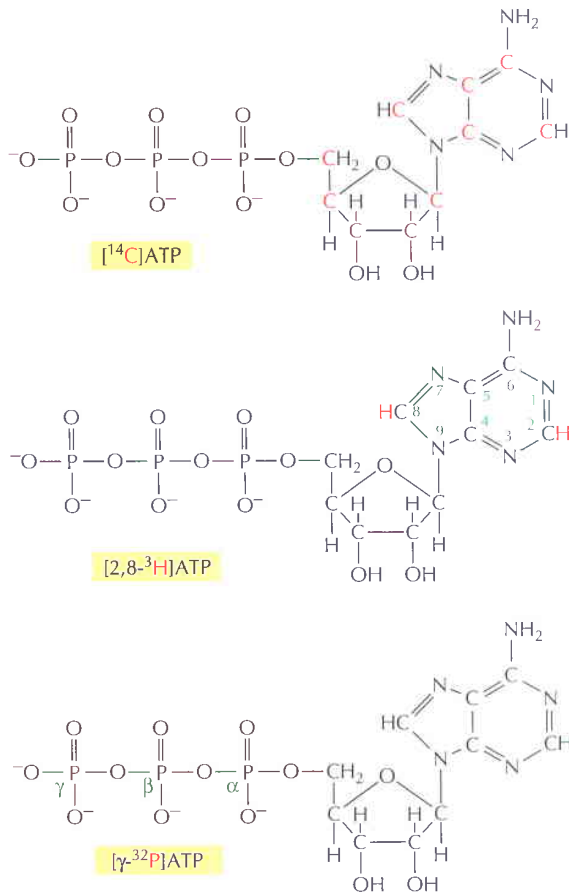


Figure 9–39 Radioisotopically labeled molecules. Three commercially available radioactive forms of ATP, with the radioactive atoms shown in red. The nomenclature used to identify the position and type of the radioactive atoms is also shown.

and remains there (**Figure 9–40**). By contrast, if cells are exposed to ^3H -uridine, a radioactive precursor of RNA, it is found that RNA is initially made in the nucleus (see Figure 4–62) and then moves rapidly into the cytoplasm. Radiolabeled molecules can also be detected by autoradiography after they are separated from other molecules by gel electrophoresis: the positions of both proteins (see Figure 8–23) and nucleic acids (see Figure 8–33A) are commonly detected on gels in this way.

Summary

Many light-microscope techniques are available for observing cells. Cells that have been fixed and stained can be studied in a conventional light microscope, whereas antibodies coupled to fluorescent dyes can be used to locate specific molecules in cells in a fluorescence microscope. Living cells can be seen with phase-contrast, differential-interference-contrast, dark-field, or bright-field microscopes. All forms of light microscopy are facilitated by digital image-processing techniques, which enhance sensitivity and refine the image. Confocal microscopy and image deconvolution both provide thin optical sections and can be used to reconstruct three-dimensional images.

Techniques are now available for detecting, measuring, and following almost any desired molecule in a living cell. Fluorescent indicator dyes can be introduced to measure the concentrations of specific ions in individual cells or in different parts of a cell. Fluorescent proteins are especially versatile probes that can be attached to other proteins by genetic manipulation. Virtually any protein of interest can be genetically engineered as a fluorescent-fusion protein, and then imaged in living cells by fluorescence microscopy. The dynamic behavior and interactions of many molecules can now be followed in living cells by variations on the use of fluorescent protein tags, in some cases at the level of single molecules. Radioactive isotopes of various elements can also be used to follow the fate of specific molecules both biochemically and microscopically.



Figure 9–40 Autoradiography. This tissue has been exposed for a short period to ^3H -thymidine. Cells that are replicating their DNA incorporate this radioactively labeled DNA precursor into their nuclei and can subsequently be visualized by autoradiography. The silver grains, seen here as black dots in the photographic emulsion over the section, reveal which cell was making new DNA. The labeled nucleus shown here is in the sensory epithelium from the inner ear of a chicken. (Courtesy of Mark Warchol and Jeffrey Corwin.)

LOOKING AT CELLS AND MOLECULES IN THE ELECTRON MICROSCOPE

Light microscopy is limited in the fineness of detail that it can reveal. Microscopes using other types of radiation—in particular, electron microscopes—can resolve much smaller structures than is possible with visible light. This higher resolution comes at a cost: specimen preparation for electron microscopy is much more complex and it is harder to be sure that what we see in the image corresponds precisely to the actual structure being examined. It is now possible, however, to use very rapid freezing to preserve structures faithfully for electron microscopy. Digital image analysis can be used to reconstruct three-dimensional objects by combining information either from many individual particles or from multiple tilted views of a single object. Together these approaches are extending the resolution and scope of electron microscopy to the point at which we can begin to faithfully image the structures of individual macromolecules and the complexes they form.

The Electron Microscope Resolves the Fine Structure of the Cell

The relationship between the limit of resolution and the wavelength of the illuminating radiation (see Figure 9–6) holds true for any form of radiation, whether it is a beam of light or a beam of electrons. With electrons, however, the limit of resolution can be made very small. The wavelength of an electron decreases as its velocity increases. In an **electron microscope** with an accelerating voltage of 100,000 V, the wavelength of an electron is 0.004 nm. In theory the resolution of such a microscope should be about 0.002 nm, which is 100,000 times that of the light microscope. Because the aberrations of an electron lens are considerably harder to correct than those of a glass lens, however, the practical resolving power of most modern electron microscopes is, at best, 0.1 nm (1 Å) (Figure 9–41). This is because only the very center of the electron lenses can be used, and the effective numerical aperture is tiny. Furthermore, problems of specimen preparation, contrast, and radiation damage have generally limited the normal effective resolution for biological objects to 1 nm (10 Å). This is nonetheless about 200 times better than the resolution of the light microscope. Moreover, in recent years, the performance of electron microscopes has been improved by the development of electron illumination sources called field emission guns. These very bright and coherent sources can substantially improve the resolution achieved.

In overall design the transmission electron microscope (TEM) is similar to a light microscope, although it is much larger and “upside down” (Figure 9–42).

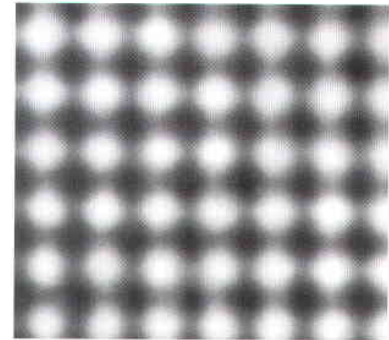


Figure 9–41 The limit of resolution of the electron microscope. This transmission electron micrograph of a thin layer of gold shows the individual files of atoms in the crystal as bright spots. The distance between adjacent files of gold atoms is about 0.2 nm (2 Å). (Courtesy of Graham Hills.)

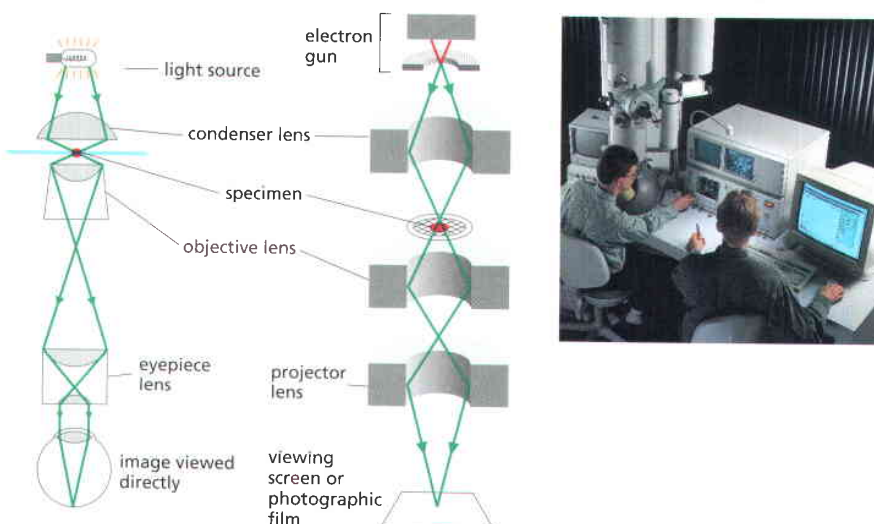


Figure 9–42 The principal features of a light microscope and a transmission electron microscope. These drawings emphasize the similarities of overall design. Whereas the lenses in the light microscope are made of glass, those in the electron microscope are magnetic coils. The electron microscope requires that the specimen be placed in a vacuum. The inset shows a transmission electron microscope in use. (Photograph courtesy of FEI Company Ltd.)

The source of illumination is a filament or cathode that emits electrons at the top of a cylindrical column about 2 m high. Since electrons are scattered by collisions with air molecules, air must first be pumped out of the column to create a vacuum. The electrons are then accelerated from the filament by a nearby anode and allowed to pass through a tiny hole to form an electron beam that travels down the column. Magnetic coils placed at intervals along the column focus the electron beam, just as glass lenses focus the light in a light microscope. The specimen is put into the vacuum, through an airlock, into the path of the electron beam. As in light microscopy, the specimen is usually stained—in this case, with *electron-dense* material, as we see in the next section. Some of the electrons passing through the specimen are scattered by structures stained with the electron-dense material; the remainder are focused to form an image, in a manner analogous to the way an image is formed in a light microscope. The image can be observed on a phosphorescent screen or recorded, either on a photographic plate or with a high-resolution digital camera. Because the scattered electrons are lost from the beam, the dense regions of the specimen show up in the image as areas of reduced electron flux, which look dark.

Biological Specimens Require Special Preparation for the Electron Microscope

In the early days of its application to biological materials, the electron microscope revealed many previously unimagined structures in cells. But before these discoveries could be made, electron microscopists had to develop new procedures for embedding, cutting, and staining tissues.

Since the specimen is exposed to a very high vacuum in the electron microscope, living tissue is usually killed and preserved by fixation—first with *glutaraldehyde*, which covalently cross-links protein molecules to their neighbors, and then with *osmium tetroxide*, which binds to and stabilizes lipid bilayers as well as proteins (Figure 9–43). Because electrons have very limited penetrating power, the fixed tissues normally have to be cut into extremely thin sections (50–100 nm thick, about 1/200 the thickness of a single cell) before they are viewed. This is achieved by dehydrating the specimen and permeating it with a monomeric resin that polymerizes to form a solid block of plastic; the block is then cut with a fine glass or diamond knife on a special microtome. These *thin sections*, free of water and other volatile solvents, are placed on a small circular metal grid for viewing in the microscope (Figure 9–44). <AAC>

The steps required to prepare biological material for viewing in the electron microscope have challenged electron microscopists from the beginning. How can we be sure that the image of the fixed, dehydrated, resin-embedded specimen finally seen bears any relation to the delicate aqueous biological system that was originally present in the living cell? The best current approaches to this problem depend on rapid freezing. If an aqueous system is cooled fast enough to a low enough temperature, the water and other components in it do not have time to rearrange themselves or crystallize into ice. Instead, the water is super-cooled into a rigid but noncrystalline state—a “glass”—called vitreous ice. This state can be achieved by slamming the specimen onto a polished copper block cooled by liquid helium, by plunging it into or spraying it with a jet of a coolant such as liquid propane, or by cooling it at high pressure.

Some frozen specimens can be examined directly in the electron microscope using a special, cooled specimen holder. In other cases the frozen block can be fractured to reveal interior surfaces, or the surrounding ice can be sublimed away to expose external surfaces. However, we often want to examine thin sections, and stain them to yield adequate contrast in the electron microscope image (discussed further below). A compromise is therefore to rapid-freeze the tissue, then replace the water, maintained in the vitreous (glassy) state, by organic solvents, and finally embed the tissue in plastic resin, cut sections, and stain. Although technically still difficult, this approach stabilizes and preserves the tissue in a condition very close to its original living state (Figure 9–45).

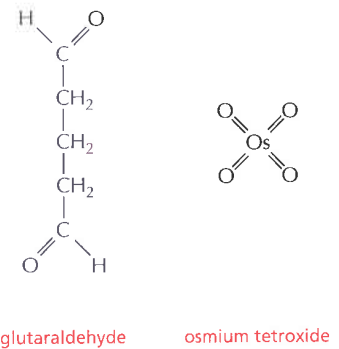


Figure 9–43 Two common chemical fixatives used for electron microscopy. The two reactive aldehyde groups of glutaraldehyde enable it to cross-link various types of molecules, forming covalent bonds between them. Osmium tetroxide forms cross-linked complexes with many organic compounds, and in the process becomes reduced. This reaction is especially useful for fixing cell membranes, since the C=C double bonds present in many fatty acids react with osmium tetroxide.

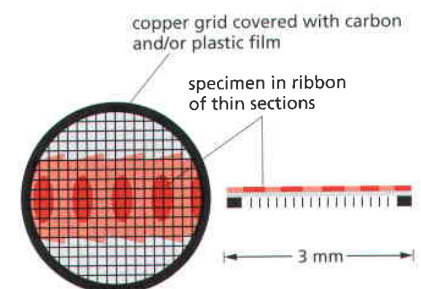


Figure 9–44 The copper grid that supports the thin sections of a specimen in a TEM.

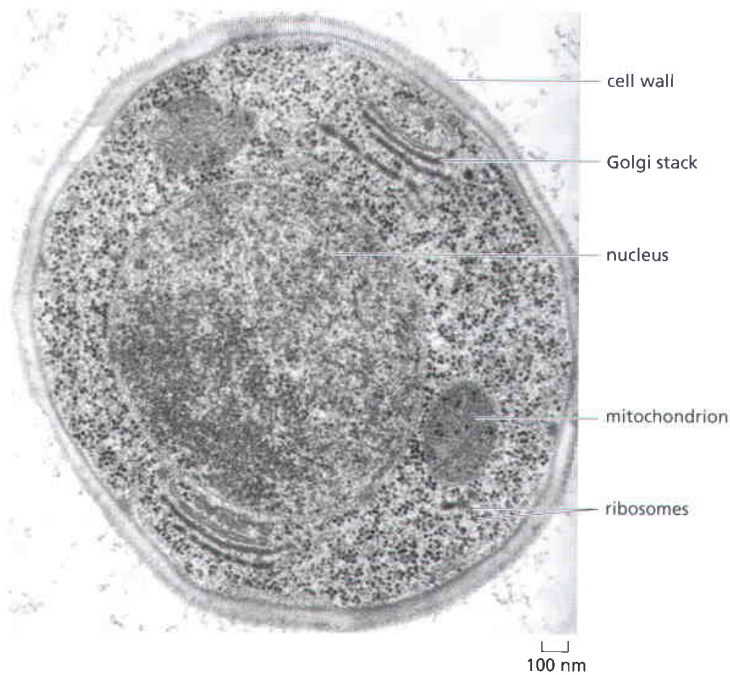


Figure 9–45 Thin section of a cell. This thin section is of a yeast cell that has been very rapidly frozen and the vitreous ice replaced by organic solvents and then by plastic resin. The nucleus, mitochondria, cell wall, Golgi stacks, and ribosomes can all be readily seen in a state that is presumed to be as life-like as possible. (Courtesy of Andrew Staehelin.)

Contrast in the electron microscope depends on the atomic number of the atoms in the specimen: the higher the atomic number, the more electrons are scattered and the greater the contrast. Biological tissues are composed of atoms of very low atomic number (mainly carbon, oxygen, nitrogen, and hydrogen). To make them visible, they are usually impregnated (before or after sectioning) with the salts of heavy metals such as uranium and lead. The degree of impregnation, or “staining,” with these salts reveals different cellular constituents with various degrees of contrast. Lipids, for example, tend to stain darkly after osmium fixation, revealing the location of cell membranes.

Specific Macromolecules Can Be Localized by Immunogold Electron Microscopy

We have seen how antibodies can be used in conjunction with fluorescence microscopy to localize specific macromolecules. An analogous method—**immunogold electron microscopy**—can be used in the electron microscope. The usual procedure is to incubate a thin section with a specific primary antibody, and then with a secondary antibody to which a colloidal gold particle has been attached. The gold particle is electron-dense and can be seen as a black dot in the electron microscope (**Figure 9–46**).

Thin sections often fail to convey the three-dimensional arrangement of cellular components in the TEM and can be very misleading: a linear structure such as a microtubule may appear in section as a pointlike object, for example, and a section through protruding parts of a single irregularly shaped solid body may give the appearance of two or more separate objects. The third dimension can be reconstructed from serial sections (**Figure 9–47**), but this is still a lengthy and tedious process.

Even thin sections, however, have a significant depth compared with the resolution of the electron microscope, so they can also be misleading in an opposite way. The optical design of the electron microscope—the very small aperture used—produces a large depth of field, so the image seen corresponds to a superimposition (a projection) of the structures at different depths. A further complication for immunogold labeling is that the antibodies and colloidal gold particles do not penetrate into the resin used for embedding; therefore, they detect antigens only at the surface of the section. This means that first, the sensitivity of detection is low, since antigen molecules present in the deeper parts of the

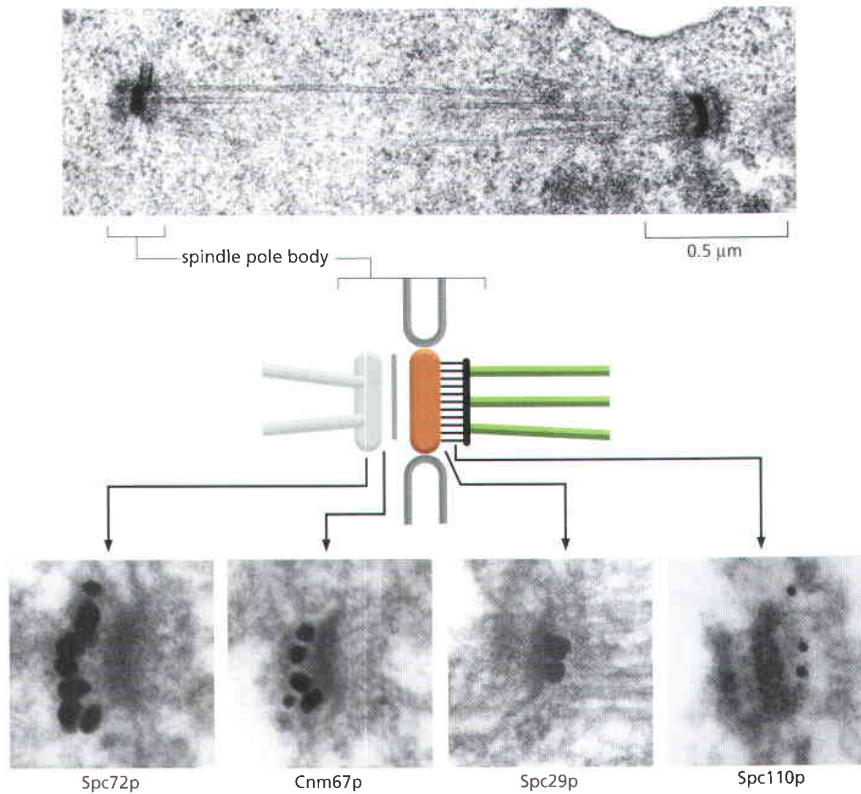


Figure 9-46 Localizing proteins in the electron microscope. Immunogold electron microscopy is used here to localize four different protein components to particular locations within the spindle pole body of yeast. At the top is a thin section of a yeast mitotic spindle showing the spindle microtubules that cross the nucleus, and connect at each end to spindle pole bodies embedded in the nuclear envelope. A diagram of the components of a single spindle pole body is shown below. Antibodies against four different proteins of the spindle pole body are used, together with colloidal gold particles (*black dots*), to reveal where within the complex structure each protein is located. (Courtesy of John Kilmartin.)

section are not detected, and second, we may get a false impression of which structures contain the antigen and which do not. A solution to this problem is to label the specimen before embedding it in plastic, when cells and tissues are still fully accessible to labeling reagents. Extremely small gold particles, about 1 nm in diameter, work best for this procedure. Such small gold particles are usually not directly visible in the final sections, so additional silver or gold is nucleated around the tiny 1 nm gold particles in a chemical process very much like photographic development.

Images of Surfaces Can Be Obtained by Scanning Electron Microscopy

A **scanning electron microscope (SEM)** directly produces an image of the three-dimensional structure of the surface of a specimen. The SEM is usually a smaller, simpler, and cheaper device than a transmission electron microscope. Whereas the TEM uses the electrons that have passed through the specimen to form an

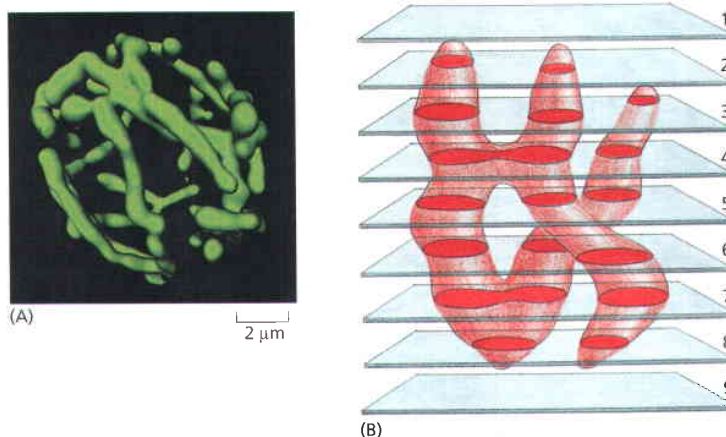


Figure 9-47 A three-dimensional reconstruction from serial sections. (A) A three-dimensional reconstruction of the mitochondrial compartment of a live yeast cell, assembled from a stack of optical sections, shows its complex branching structure. Single thin sections of such a structure in the electron microscope sometimes give misleading impressions. In this example (B), most sections through a cell containing a branched mitochondrion seem to contain two or three separate mitochondria (compare Figure 9-45). Sections 4 and 7, moreover, might be interpreted as showing a mitochondrion in the process of dividing. The true three-dimensional shape, however, can be reconstructed from serial sections. (A, courtesy of Stefan Hell.)

image, the SEM uses electrons that are scattered or emitted from the specimen's surface. The specimen to be examined is fixed, dried, and coated with a thin layer of heavy metal. Alternatively, it can be rapidly frozen, and then transferred to a cooled specimen stage for direct examination in the microscope. Often an entire plant part or small animal can be put into the microscope with very little preparation (Figure 9–48). The specimen, prepared in any of these ways, is then scanned with a very narrow beam of electrons. The quantity of electrons scattered or emitted as this primary beam bombards each successive point of the metallic surface is measured and used to control the intensity of a second beam, which moves in synchrony with the primary beam and forms an image on a television screen. In this way, a highly enlarged image of the surface as a whole is built up (Figure 9–49).

The SEM technique provides great depth of field; moreover, since the amount of electron scattering depends on the angle of the surface relative to the beam, the image has highlights and shadows that give it a three-dimensional appearance (see Figure 9–48 and Figure 9–50). Only surface features can be examined, however, and in most forms of SEM, the resolution attainable is not very high (about 10 nm, with an effective magnification of up to 20,000 times). As a result, the technique is usually used to study whole cells and tissues rather than subcellular organelles. <AACG> Very high-resolution SEMs have, however, been developed with a bright coherent-field emission gun as the electron source. This type of SEM can produce images that rival TEM images in resolution (Figure 9–51).

Metal Shadowing Allows Surface Features to Be Examined at High Resolution by Transmission Electron Microscopy

The TEM can also be used to study the surface of a specimen—and generally at a higher resolution than in the SEM—to reveal the shape of individual macromolecules for example. As in scanning electron microscopy, a thin film of a heavy metal such as platinum is evaporated onto the dried specimen. In this case, however, the metal is sprayed from an oblique angle so as to deposit a coat-

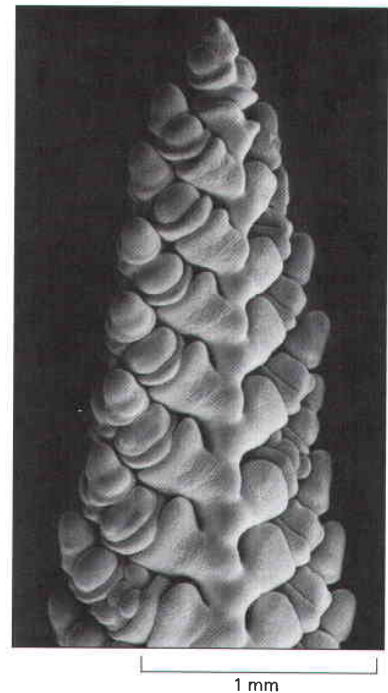


Figure 9–48 A developing wheat flower, or spike. This delicate flower spike was rapidly frozen, coated with a thin metal film, and examined in the frozen state in a SEM. This micrograph, which is at a low magnification, demonstrates the large depth of focus of the SEM. (Courtesy of Kim Findlay.)

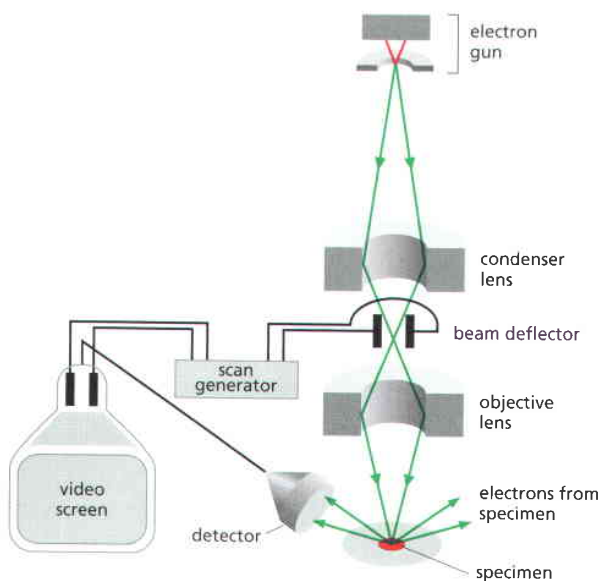


Figure 9–49 The scanning electron microscope. In a SEM, the specimen is scanned by a beam of electrons brought to a focus on the specimen by the electromagnetic coils that act as lenses. The detector measures the quantity of electrons scattered or emitted as the beam bombards each successive point on the surface of the specimen and controls the intensity of successive points in an image built up on a video screen. The SEM creates striking images of three-dimensional objects with great depth of focus and a resolution between 3 nm and 20 nm depending on the instrument. (Photograph courtesy of Andrew Davies.)

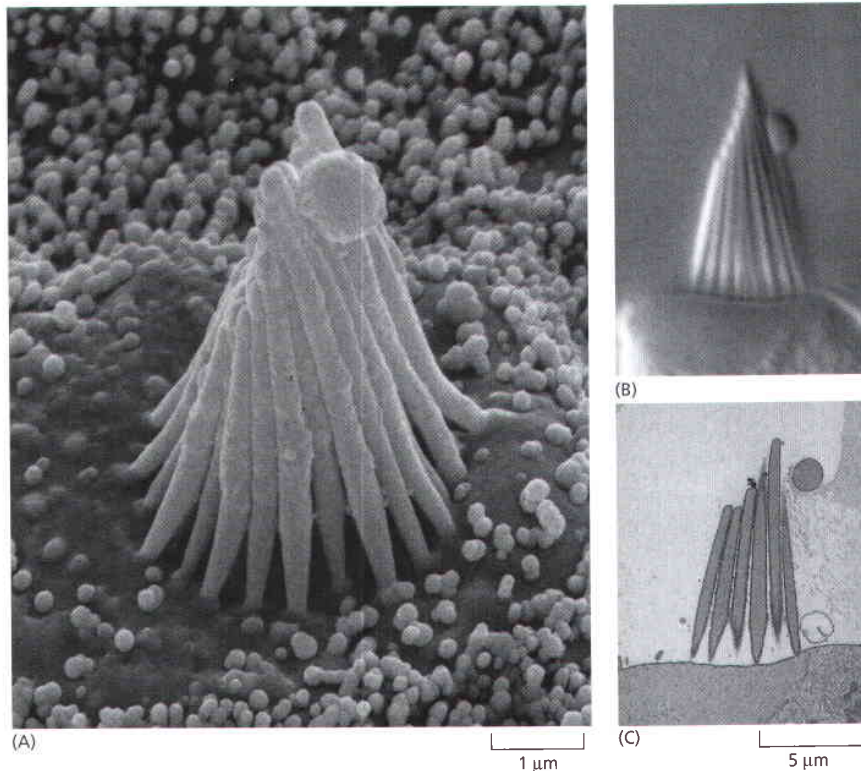


Figure 9-50 Scanning electron microscopy. (A) A scanning electron micrograph of the stereocilia projecting from a hair cell in the inner ear of a bullfrog. <CATA> For comparison, the same structure is shown by (B) differential-interference-contrast light microscopy and (C) thin-section transmission electron microscopy. (Courtesy of Richard Jacobs and James Hudspeth.)

ing that is thicker in some places than others—a process known as *metal shadowing* because a shadow effect is created that gives the image a three-dimensional appearance.

Some specimens coated in this way are thin enough or small enough for the electron beam to penetrate them directly. This is the case for individual molecules, macromolecular complexes, and viruses—all of which can be dried down, before shadowing, onto a flat supporting film made of a material that is relatively transparent to electrons, such as carbon or plastic. The internal structure of cells can also be imaged using metal shadowing. In this case samples are very rapidly frozen (as described above) and then cracked open with a knife blade. The ice level at the fractured surface is lowered by the sublimation of ice in a vacuum as the temperature is raised—in a process called freeze-drying. The parts of the cell exposed by this *etching* process are then shadowed as before to make a metal replica. The organic material of the cell remains must be dissolved away after shadowing to leave only the thin metal *replica* of the surface of the specimen. The replica is then reinforced with a film of carbon so it can be placed on a grid and examined in the transmission electron microscope in the ordinary way (Figure 9-52). This technique exposes structures in the interior of the cell and can reveal their three-dimensional organization with exceptional clarity (Figure 9-53).

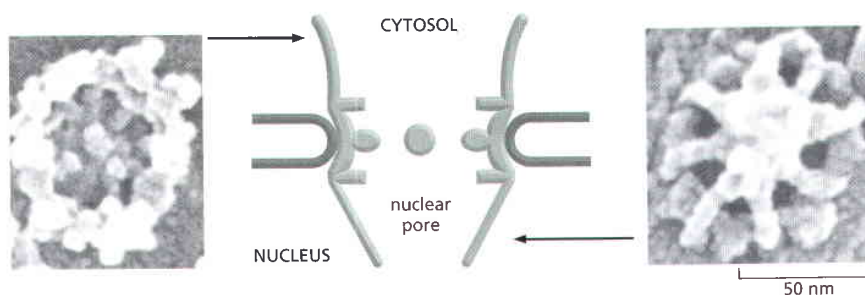


Figure 9-51 The nuclear pore. Rapidly frozen nuclear envelopes were imaged in a high-resolution SEM, equipped with a field emission gun as the source of electrons. These views of each side of a nuclear pore represent the limit of resolution of the SEM, and should be compared with Figure 12-9. (Courtesy of Martin Goldberg and Terry Allen.)

Negative Staining and Cryoelectron Microscopy Both Allow Macromolecules to Be Viewed at High Resolution

Although isolated macromolecules, such as DNA or large proteins, can be visualized readily in the electron microscope if they are shadowed with a heavy metal to provide contrast, finer detail can be seen by using **negative staining**. In this technique, the molecules, supported on a thin film of carbon, are mixed with a solution of a heavy-metal salt such as uranyl acetate. After the sample has dried, a very thin film of metal salt covers the carbon film everywhere except where it has been excluded by the presence of an adsorbed macromolecule. Because the macromolecule allows electrons to pass through it much more readily than does the surrounding heavy-metal stain, a reversed or negative image of the molecule is created. Negative staining is especially useful for viewing large macromolecular aggregates such as viruses or ribosomes, and for seeing the subunit structure of protein filaments (Figure 9-54).

Shadowing and negative staining can provide high-contrast surface views of small macromolecular assemblies, but the size of the smallest metal particles in the shadow or stain used limits the resolution of both techniques. Recent methods provide an alternative that has allowed us to visualize directly at high resolution even the interior features of three-dimensional structures such as viruses and organelles. In this technique, called **cryoelectron microscopy**, rapid freezing to form vitreous ice is again the key. A very thin (about 100 nm) film of an aqueous suspension of virus or purified macromolecular complex is prepared on a microscope grid. The specimen is then rapidly frozen by plunging it into a coolant. A special sample holder is used to keep this hydrated specimen at -160°C in the vacuum of the microscope, where it can be viewed directly without fixation, staining, or drying. Unlike negative staining, in which what we see is the envelope of stain exclusion around the particle, hydrated cryoelectron microscopy produces an image from the macromolecular structure itself. However, to extract the maximum amount of structural information, special image-processing techniques must be used, as we describe next.

Multiple Images Can Be Combined to Increase Resolution

Any image, whether produced by an electron microscope or by an optical microscope, is made by particles—electrons or photons—striking a detector of some sort. But these particles are governed by quantum mechanics, so the numbers reaching the detector are predictable only in a statistical sense. In the limit of very large numbers of particles, the distribution at the detector is accurately determined by the imaged specimen. However, with smaller numbers of particles, this underlying structure in the image is obscured by the statistical fluctuations in the numbers of particles detected in each region. The term *noise* describes the random variability that confuses the underlying image of the spec-

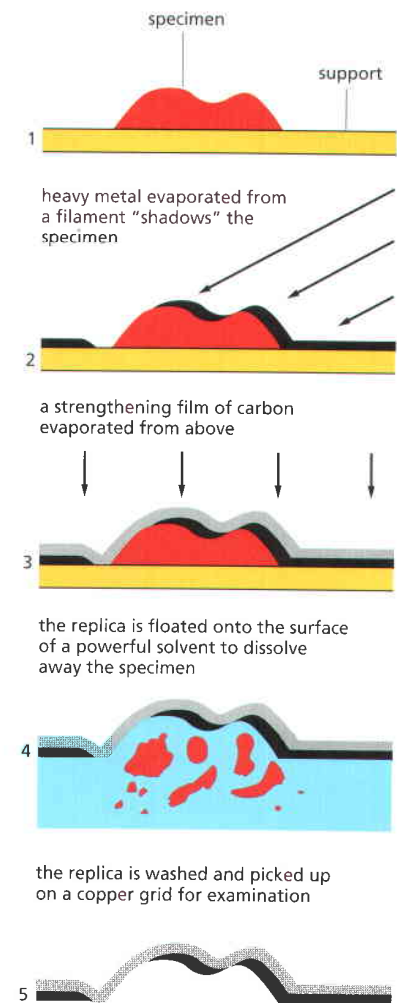
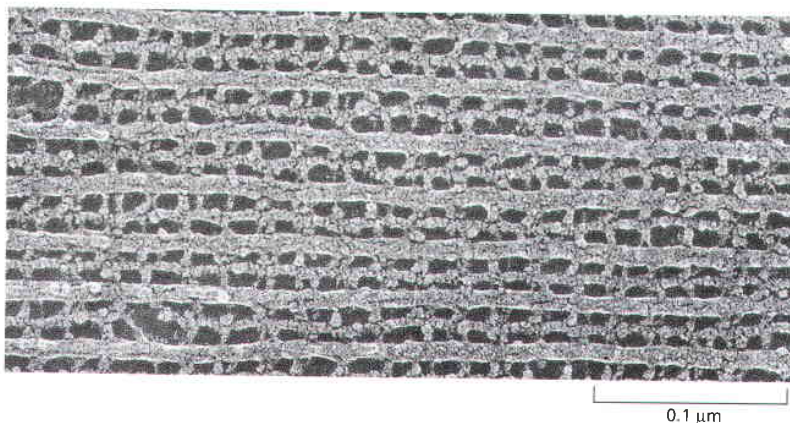


Figure 9-52 The preparation of a metal-shadowed replica of the surface of a specimen. Note that the thickness of the metal reflects the surface contours of the original specimen.

Figure 9-53 A regular array of protein filaments in an insect muscle. To obtain this image, the muscle cells were rapidly frozen to liquid helium temperature, fractured through the cytoplasm, and subjected to deep etching. A metal-shadowed replica was then prepared and examined at high magnification. (Courtesy of Roger Cooke and John Heuser.)

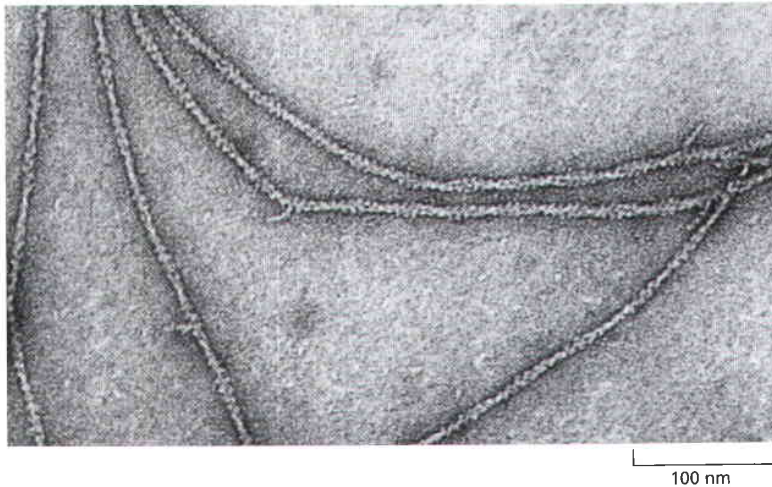


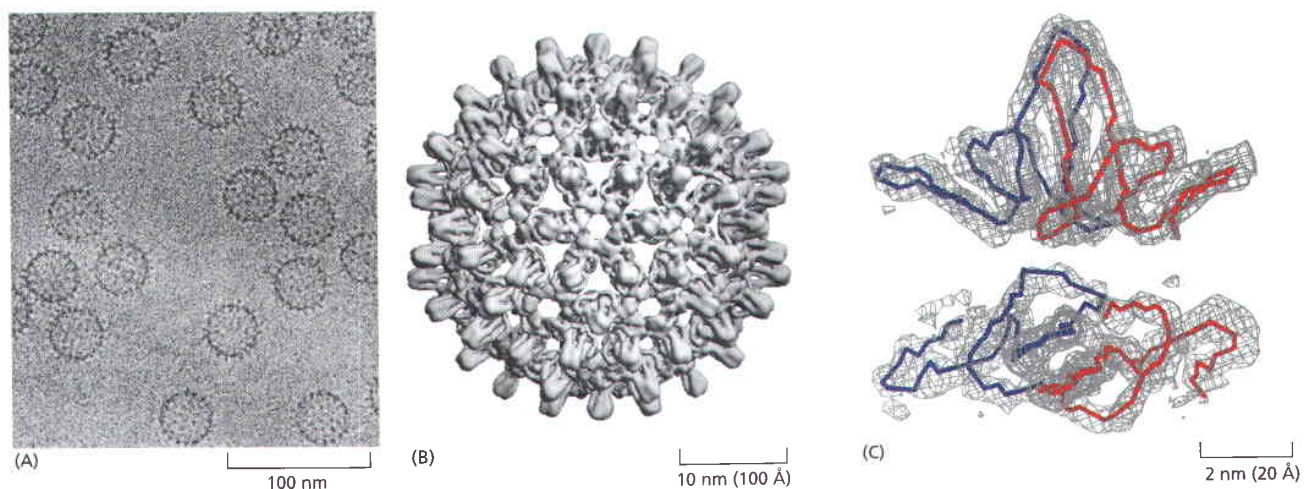
Figure 9–54 Negatively stained actin filaments. In this transmission electron micrograph, each filament is about 8 nm in diameter and is seen, on close inspection, to be composed of a helical chain of globular actin molecules. (Courtesy of Roger Craig.)

imen itself. Noise is important in light microscopy at low light levels, but it is a particularly severe problem for electron microscopy of unstained macromolecules. A protein molecule can tolerate a dose of only a few tens of electrons per square nanometer without damage, and this dose is orders of magnitude below what is needed to define an image at atomic resolution.

The solution is to obtain images of many identical molecules—perhaps tens of thousands of individual images—and combine them to produce an averaged image, revealing structural details that were hidden by the noise in the original images. This procedure is called **single-particle reconstruction**. Before combining all the individual images, however, they must be aligned with each other. Sometimes it is possible to induce proteins and complexes to form crystalline arrays, in which each molecule is held in the same orientation in a regular lattice. In this case, the alignment problem is easily solved, and several protein structures have been determined at atomic resolution by this type of electron crystallography. In principle, however, crystalline arrays are not absolutely required. With the help of a computer, the digital images of randomly distributed and unaligned molecules can be processed and combined to yield high-resolution reconstructions. Although structures that have some intrinsic symmetry make the task of alignment easier and more accurate, this technique has also been used for objects, like ribosomes, with no symmetry. **Figure 9–55** shows the structure of an icosahedral virus that has been determined at high resolution by the combination of many particles and multiple views.

With well-ordered crystalline arrays, a resolution of 0.3 nm has been achieved by electron microscopy—enough to begin to see the internal atomic

Figure 9–55 Single-particle reconstruction. Spherical protein shells of the hepatitis B virus are preserved in a thin film of ice (A) and imaged in the transmission electron microscope. Thousands of individual particles were combined by single-particle reconstruction to produce the three-dimensional map of the icosahedral particle shown in (B). The two views of a single protein dimer (C), forming the spikes on the surface of the shell, show that the resolution of the reconstruction (0.74 nm) is sufficient to resolve the complete fold of the polypeptide chain. (A, courtesy of B. Böttcher, S.A. Wynne, and R.A. Crowther; B and C, from B. Böttcher, S.A. Wynne, and R.A. Crowther, *Nature* 386:88–91, 1997. With permission from Macmillan Publishers Ltd.)



arrangements in a protein and to rival x-ray crystallography in resolution. With single-particle reconstruction, the present limit is about 0.5 nm, enough to identify protein subunits and domains, and limited protein secondary structure. Although electron microscopy is unlikely to supersede x-ray crystallography (discussed in Chapter 8) as a method for macromolecular structure determination, it has some very clear advantages. First, it does not absolutely require crystalline specimens. Second, it can deal with extremely large complexes—structures that may be too large or too variable to crystallize satisfactorily.

The analysis of large and complex macromolecular structures is helped considerably if the atomic structure of one or more of the subunits is known, for example from x-ray crystallography. Molecular models can then be mathematically “fitted” into the envelope of the structure determined at lower resolution using the electron microscope. **Figure 9–56** shows the structure of a ribosome with the location of a bound release factor displayed in this way (see also Figures 6–74 and 6–75).

Different Views of a Single Object Can Be Combined to Give a Three-dimensional Reconstruction

The detectors used to record images from electron microscopes produce two-dimensional pictures. Because of the large depth of field of the microscope, all the parts of the three-dimensional specimen are in focus, and the resulting image is a projection of the structure along the viewing direction. The lost information in the third dimension can be recovered if we have views of the same specimen from many different directions. The computational methods for this technique were worked out in the 1960s, and they are widely used in medical computed tomography (CT) scans. In a CT scan, the imaging equipment is moved around the patient to generate the different views. In **electron-microscope (EM) tomography**, the specimen holder is tilted in the microscope, which achieves the same result. In this way, we can arrive at a three-dimensional reconstruction, in a chosen standard orientation, by combining a set of different views of a single object in the microscope's field of view. Each individual view will be very noisy, but by combining them in three dimensions and taking an average, the noise can be largely eliminated, yielding a clear view of the molecular structure. Starting with thick plastic sections of embedded material, three-dimensional reconstructions, or *tomograms*, <ATCC> <CGAT> are used extensively to describe the detailed anatomy of small regions of the cell, such as the Golgi apparatus (**Figure 9–57**) or the cytoskeleton. Increasingly, however, microscopists are applying EM tomography to unstained frozen hydrated sections, and even to rapidly frozen whole cells or organelles (**Figure 9–58**). Electron microscopy now provides a robust bridge between the scale of the single molecule and that of the whole cell.

Summary

Determining the detailed structure of the membranes and organelles in cells requires the higher resolution attainable in a transmission electron microscope. Specific macromolecules can be localized with colloidal gold linked to antibodies. Three-dimensional views of the surfaces of cells and tissues are obtained by scanning electron microscopy. The shapes of isolated macromolecules that have been shadowed with a heavy metal or outlined by negative staining can also be readily determined by electron microscopy. Using computational methods, either multiple images or views from different directions can be combined to produce detailed reconstructions of macromolecules and molecular complexes through the techniques of electron tomography and single-particle reconstruction, often applied to cryo-preserved specimens. The resolution obtained with these methods means that atomic structures of individual macromolecules can often be “fitted” to the images derived by electron microscopy, and that the TEM is increasingly able to completely bridge the gap between structures determined by x-ray crystallography and those determined in the light microscope.

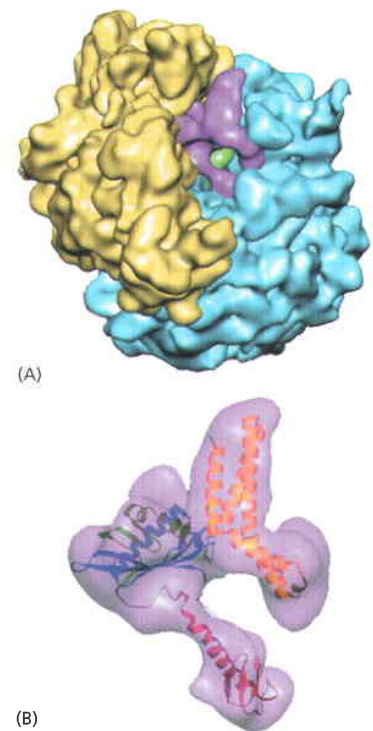


Figure 9–56 Single-particle reconstruction and molecular model fitting. Bacterial ribosomes, with and without the release factor required for peptide release from the ribosome, were used here to derive high-resolution three-dimensional cryo-EM maps at a resolution of better than 1 nm. Images of nearly 20,000 separate ribosomes, preserved in ice, were used to produce single particle reconstructions. In (A) the 30S ribosomal subunit (*yellow*) and the 50S subunit (*blue*) can be distinguished from the additional electron density that can be attributed to the release factor RF2 (*pink*). The known molecular structure of RF2 has then been modeled into this electron density (B). (From U.B.S. Rawat et al., *Nature* 421:87–90, 2003. With permission from Macmillan Publishers Ltd.)

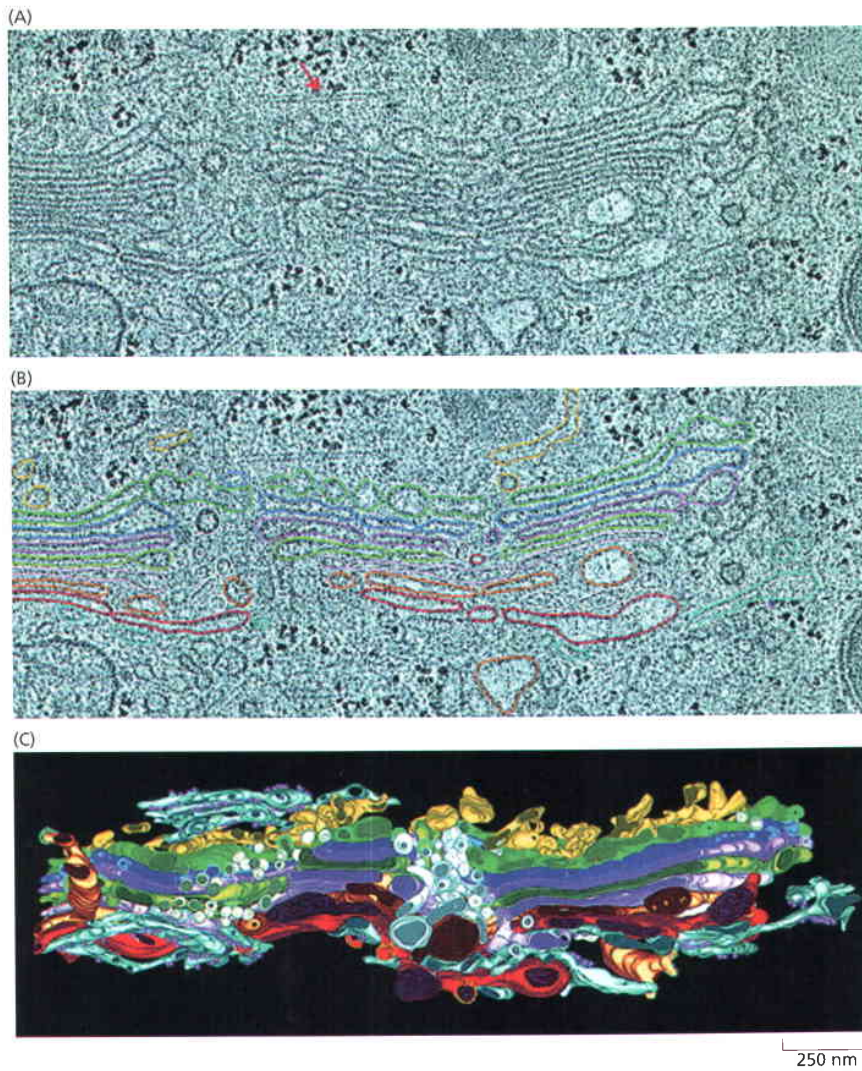


Figure 9-57 Electron microscope (EM) tomography. Samples that have been rapidly frozen, and then freeze-substituted and embedded in plastic, preserve their structure in a condition that is very close to their original living state. This experiment shows an analysis of the three-dimensional structure of the Golgi apparatus from a rat kidney cell prepared in this way. Several thick sections (250 nm) of the cell have been tilted in a high-voltage electron microscope, along two different axes, and about 160 different views recorded. The digital data were combined using EM tomography methods to produce a final three-dimensional reconstruction at a resolution of about 7 nm. The computer can then present very thin slices of the complete three-dimensional data set, or tomogram, and two serial slices, each only 4 nm thick, are shown here (A) and (B). Very little changes from one slice to the next, but using the full data set, and by manually color coding the membranes (B), a full three-dimensional picture of the complete Golgi complex and its associated vesicles can be presented (C). (From M.S. Ladinsky et al., *J. Cell Biol.* 144:1135–1149, 1999. With permission from The Rockefeller University Press.)

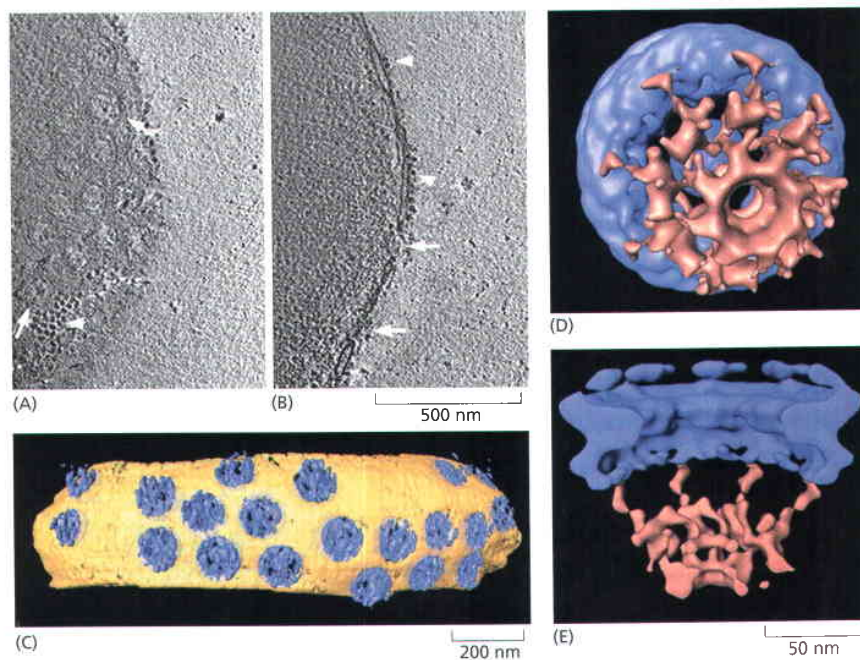


Figure 9-58 Combining cryo-EM tomography and single-particle reconstruction. In addition to sections, the technique of EM tomography may also be applied to small unfixed specimens that are rapidly frozen and examined, while still frozen, using a tilting stage in the microscope. In this experiment the small nuclei of *Dictyostelium* are gently isolated and then very rapidly frozen before a series of tilted views of them is recorded. These different digital views are combined by EM tomography methods to produce a three-dimensional tomogram. Two thin digital slices (10 nm) through this tomogram are shown, in which top views (A) and side views (B) of individual nuclear pores can be seen. In the three-dimensional model (C), a surface rendering of the pores (blue) can be seen embedded in the nuclear envelope (yellow). From a series of tomograms it was possible to extract data sets for nearly 300 separate nuclear pores, whose structures could then be averaged using the techniques of single particle reconstruction. The surface-rendered view of one of these reconstructed pores is shown from the nuclear face in (D) and in section in (E) and should be compared with Figure 12-10. The pore complex is colored blue and the nuclear basket brown. (From M. Beck et al., *Science* 306:1387–1390, 2004. With permission from AAAS.)

PROBLEMS

Which statements are true? Explain why or why not.

9-1 Because the DNA double helix is only 10 nm wide—well below the resolution of the light microscope—it is impossible to see chromosomes in living cells without special stains.

9-2 A fluorescent molecule, having absorbed a single photon of light at one wavelength, always emits it at a longer wavelength.

9-3 Caged molecules can be introduced into a cell and then activated by a strong pulse of laser light at the precise time and cellular location chosen by the experimenter.

Discuss the following problems.

9-4 The diagrams in **Figure Q9-1** show the paths of light rays passing through a specimen with a dry lens and with an oil-immersion lens. Offer an explanation for why oil-immersion lenses should give better resolution. Air, glass, and oil have refractive indices of 1.00, 1.51, and 1.51, respectively.

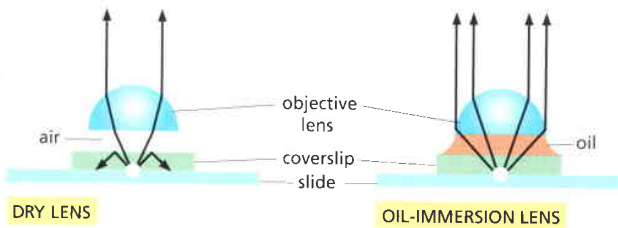


Figure Q9-1 Paths of light rays through dry and oil-immersion lenses (Problem 9-4). The white circle at the origin of the light rays is the specimen.

9-5 **Figure Q9-2** shows a diagram of the human eye. The refractive indices of the components in the light path are: cornea 1.38, aqueous humor 1.33, crystalline lens 1.41, and vitreous humor 1.38. Where does the main refraction—the main focusing—occur? What role do you suppose the lens plays?

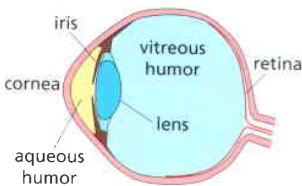


Figure Q9-2 Diagram of the human eye (Problem 9-5).

9-6 Why do humans see so poorly underwater? And why do goggles help?

9-7 Explain the difference between resolution and magnification.

9-8 Antibodies that bind to specific proteins are important tools for defining the locations of molecules in cells. The sensitivity of the primary antibody—the antibody that reacts with the target molecule—is often enhanced by using labeled secondary antibodies that bind to it. What are the advantages and disadvantages of using secondary antibodies that carry fluorescent tags versus those that carry bound enzymes?

9-9 **Figure Q9-3** shows a series of modified GFPs that emit light in a range of colors. How do you suppose the exact same chromophore can fluoresce at so many different wavelengths?

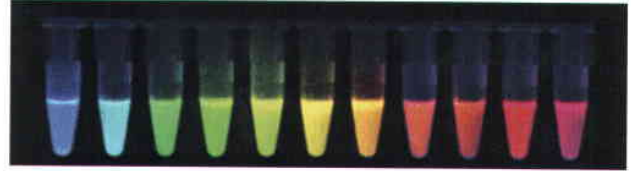


Figure Q9-3 A rainbow of colors produced by modified GFPs (Problem 9-9). (From R.F. Service, *Science* 306:1457, 2004. With permission from AAAS.)

9-10 Consider a fluorescent detector designed to report the cellular location of active protein tyrosine kinases. A blue (cyan) fluorescent protein (CFP) and a yellow fluorescent protein (YFP) were fused to either end of a hybrid protein domain. The hybrid protein segment consisted of a substrate peptide recognized by the Abl protein tyrosine kinase and a phosphotyrosine binding domain (**Figure Q9-4A**). Stimulation of the CFP domain does not cause emission by the YFP domain when the domains are separated. When the CFP and YFP domains are brought close together, however, fluorescence resonance energy transfer (FRET) allows excitation of CFP to stimulate emission by YFP. FRET shows up experimentally as an increase in the ratio of emission at 526 nm versus 476 nm (YFP/CFP) when CFP is excited by 434-nm light.

Incubation of the reporter protein with Abl protein tyrosine kinase in the presence of ATP gave an increase in YFP/CFP emission (**Figure Q9-4B**). In the absence of ATP or the Abl protein, no FRET occurred. FRET was also eliminated by addition of a tyrosine phosphatase (**Figure Q9-4B**). Describe as best you can how the reporter protein detects active Abl protein tyrosine kinase.

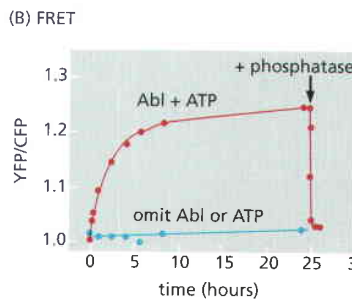
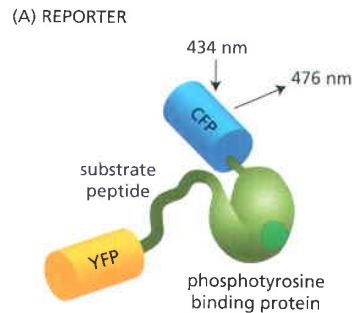


Figure Q9-4 Fluorescent reporter protein designed to detect tyrosine phosphorylation (Problem 9-10). (A) Domain structure of reporter protein. Four domains are indicated: CFP, YFP, tyrosine kinase substrate peptide, and a phosphotyrosine-binding domain. (B) FRET assay. YFP/CFP is normalized to 1.0 at time zero. The reporter was incubated in the presence (or absence) of Abl and ATP for the indicated times. Arrow indicates time of addition of a tyrosine phosphatase. (From A.Y. Ting, K.H. Klain, R.L. Klemke and R.Y. Tsien, *Proc. Natl Acad. Sci. U.S.A.* 98:15003–15008, 2001. With permission from National Academy of Sciences.)

9-11 The practical resolving power of modern electron microscopes is around 0.1 nm. The major reason for this constraint is the small numerical aperture ($n \sin \theta$), which is

limited by θ (half the angular width of rays collected at the objective lens). Assuming that the wavelength (λ) of the electron is 0.004 nm and that the refractive index (n) is 1.0, calculate the value for θ . How does that value compare with a θ of 60°, which is typical for light microscopes?

$$\text{resolution} = \frac{0.61 \lambda}{n \sin \theta}$$

9–12 It is difficult to tell bumps from pits just by looking at the pattern of shadows. Consider **Figure Q9–5**, which shows a set of shaded circles. In **Figure Q9–5A** the circles appear to be bumps; however, when the picture is simply turned upside down (**Figure Q9–5B**), the circles seem to be pits. This is a classic illusion. The same illusion is present in metal shadowing, as shown in the two electron micrographs in **Figure Q9–5**. In one the membrane appears to be covered in bumps, while in the other the membrane looks heavily pitted. Is it possible for an electron microscopist to be sure that one view is correct, or is it all arbitrary? Explain your reasoning.

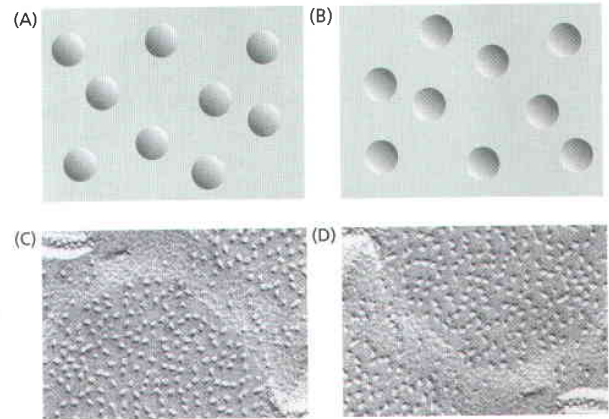


Figure Q9–5 Bumps and pits (Problem 9–12). (A) Shaded circles that look like bumps. (B) Shaded circles that look like pits. (C) An electron micrograph oriented so that it appears to be covered with bumps. (D) An electron micrograph oriented so that it appears to be covered with pits. (C and D, courtesy of Andrew Staehelin.)

REFERENCES

General

- Celis JE, Carter N, Simons K et al (eds) (2005) *Cell Biology: A Laboratory Handbook*, 3rd ed. San Diego: Academic Press. (Volume 3 of this four volume set covers the practicalities of most of the current light and electron imaging methods that are used in cell biology, while volume 4 covers the transfer of molecules into cells.)
- Pawley BP (ed) (2006) *Handbook of Biological Confocal Microscopy*, 3rd ed. New York: Springer Science.

Looking at Cells in the Light Microscope

- Adams MC, Salmon WC, Gupton SL et al (2003) A high-speed multispectral spinning-disk confocal microscope system for fluorescent speckle microscopy of living cells. *Methods* 29:29–41.
- Agard DA, Hiraoka Y, Shaw P & Sedat JW (1989) Fluorescence microscopy in three dimensions. In *Methods in Cell Biology*, vol 30: Fluorescence Microscopy of Living Cells in Culture, part B (DL Taylor, Y-L Wang eds), San Diego: Academic Press.
- Centonze VE (2002) Introduction to multiphoton excitation imaging for the biological sciences. *Methods Cell Biol* 70:129–48.
- Chalfie M, Tu Y, Euskirchen G et al (1994) Green fluorescent protein as a marker for gene expression. *Science* 263:802–805.
- Giepmans BN, Adams SR, Ellisman MH & Tsien RY (2006) The fluorescent toolbox for assessing protein location and function. *Science* 312:217–224.
- Harlow E & Lane D (1988) *Antibodies*. A Laboratory Manual. Cold Spring Harbor, NY: Cold Spring Harbor Laboratory Press.
- Haugland RP (ed) (1996) *Handbook of Fluorescent Probes and Research Chemicals*, 8th ed. Eugene, OR: Molecular Probes, Inc. (Available online at <http://www.probes.com/>)
- Jaiswai JK & Simon SM (2004) Potentials and pitfalls of fluorescent quantum dots for biological imaging. *Trends Cell Biol* 14:497–504.
- Jares-Erijman EA & Jovin TM (2003) FRET imaging. *Nature Biotech* 21:1387–1395.
- Lippincott-Shwartz J, Altan-Bonnet N & Patterson G (2003) Photobleaching and photoactivation: following protein dynamics in living cells. *Nature Cell Biol* 5:S7–S14.
- Minsky M (1988) Memoir on inventing the confocal scanning microscope. *Scanning* 10:128–138.
- Miyawaki A, Sawano A & Kogure T (2003) Lighting up cells: labeling proteins with fluorophores. *Nature Cell Biol* 5:S1–S7.
- Parton RM & Read ND (1999) Calcium and pH imaging in living cells. In *Light Microscopy in Biology*, A Practical Approach, 2nd ed. (Lacey AJ ed) Oxford: Oxford University Press.
- Sako Y & Yanagida T (2003) Single-molecule visualization in cell biology. *Nature Rev Mol Cell Biol* 4:SS1–SS5.

- Sekar RB & Periasamy A (2003) Fluorescence resonance energy transfer (FRET) microscopy imaging of live cell protein localizations. *J Cell Biol* 160:629–633.
- Shaner NC, Steinbach PA & Tsien RY (2005) A guide to choosing fluorescent proteins. *Nature Methods* 2:905–909.
- Sheetz MP (ed) (1997) *Laser Tweezers in Cell Biology*. *Methods Cell Biol* 55.
- Sluder G & Wolf DE (2007) *Video Microscopy* 3rd ed. *Methods Cell Biol* 81.
- Stevens DJ & Allan (2003) *Light Microscopy Techniques for Live Cell Imaging*. *Science* 300:82–86.
- Tsien RY (2003) Imagining imaging's future. *Nature Rev Mol Cell Rev* 4:SS16–SS21.
- Weiss DG, Maile W, Wick RA & Steffen W (1999) Video microscopy. In *Light Microscopy in Biology: A Practical Approach*, 2nd ed. (AJ Lacey ed) Oxford: Oxford University Press.
- White JG, Amos WB & Fordham M (1987) An evaluation of confocal versus conventional imaging of biological structures by fluorescence light microscopy. *J Cell Biol* 105:41–48.
- Zernike F (1955) How I discovered phase contrast. *Science* 121:345–349.

Looking at Cells and Molecules in the Electron Microscope

- Allen TD & Goldberg MW (1993) High resolution SEM in cell biology. *Trends Cell Biol* 3:203–208.
- Baumeister W (2002) Electron tomography: towards visualizing the molecular organization of the cytoplasm. *Curr Opin Struct Biol* 12:679–684.
- Böttcher B, Wynne SA & Crowther RA (1997) Determination of the fold of the core protein of hepatitis B virus by electron cryomicroscopy. *Nature* 386:88–91.
- Dubochet J, Adrian M, Chang J-J et al (1988) Cryoelectron microscopy of vitrified specimens. *Q Rev Biophys* 21:129–228.
- Frank J (2003) Electron microscopy of functional ribosome complexes. *Biopolymers* 68:223–233.
- Hayat MA (2000) *Principles and Techniques of Electron Microscopy*, 4th ed. Cambridge: Cambridge University Press.
- Heuser J (1981) Quick-freeze, deep-etch preparation of samples for 3D electron microscopy. *Trends Biochem Sci* 6:64–68.
- Lippincott-Schwartz J & Patterson GH (2003) Development and use of fluorescent protein markers in living cells. *Science* 300:87–91.
- McIntosh R, Nicastro D & Mastrorarde D (2005) New views of cells in 3D: an introduction to electron tomography. *Trends Cell Biol* 15:43–51.
- McDonald KL & Auer M (2006) High pressure freezing, cellular tomography, and structural cell biology. *Biotechniques* 41:137–139.
- Pease DC & Porter KR (1981) Electron microscopy and ultramicrotomy. *J Cell Biol* 91:287s–292s.
- Unwin PNT & Henderson R (1975) Molecular structure determination by electron microscopy of unstained crystal specimens. *J Mol Biol* 94:425–440.